Marine Geology 357 (2014) 362–383

Contents lists available at ScienceDirect

Marine Geology

journal homepage: www.elsevier.com/locate/margeo

Classification of submarine canyons of the Australian continental margin

Zhi Huang [a,*], Scott L. Nichol [a], Peter T. Harris [b], M. Julian Caley [c]

[a] Geoscience Australia, GPO Box 378, Canberra, ACT 2601, Australia
[b] GRID-Arendal, PO Box 183, N-4802 Arendal, Norway
[c] Australian Institute of Marine Science, PMB 3, Townsville MC, Queensland 4810, Australia

ARTICLE INFO

Article history:
Received 11 February 2014
Received in revised form 22 July 2014
Accepted 24 July 2014
Available online 1 August 2014

Keywords:
Australia
submarine canyons
bathymetry
morphometrics
hierarchical classification

ABSTRACT

Submarine canyons influence oceanographic processes, sediment transport, productivity and benthic biodiversity from the continental shelf to the slope and beyond. However, not all canyons perform the same function. The relative influence of an individual canyon on these processes will, in part, be determined by its form, shape and position on the continental margin. Here we present an analysis of canyon geomorphic metrics using an updated national dataset of 713 submarine canyons surrounding mainland Australia. These metrics (attributes) for each canyon are used to classify them into canyon types across a hierarchy of physical characteristics separately for shelf-incising ($n = 95$) and slope-confined (blind; $n = 618$) canyons. We find that the canyon metrics describe a wide variety of canyon form and complexity that is consistent with a population of canyons that has evolved at different rates around the Australian margin since the break-up of Gondwana. The large number of slope-confined canyons is interpreted to reflect dominance of slope mass-wasting processes over erosive turbidity flows from fluvial and shelf sources on an arid continent. The distribution of submarine canyons around the Australian margin is not regular, with clusters occurring in the east, southeast, west and southwest where the margin is steepest. The classification result provides a quantitative framework for describing canyon heterogeneity for application in studies of geological controls on individual canyons, canyon oceanography and canyon biodiversity.

1. Introduction

Submarine canyons are common geomorphic features that occur on the margins of all continents (Shepard, 1972; Harris and Whiteway, 2011; Harris et al., 2014). Their complex morphology interacts with ocean currents, tides and internal waves, setting up hydrodynamic conditions that influence benthic ecosystems and habitats (Vetter, 1994; Bosley et al., 2004; De Leo et al., 2010). Submarine canyons were first scientifically described by marine geologists, who focused on their significance as major geomorphic features of continental margins and as conduits for sediment export from coastal and shelf environments to the deep sea over geologic timescales (e.g. Shepard and Dill, 1966). More recently, the ecological significance of submarine canyons has been recognised, as features associated with enhanced primary productivity, benthic biomass and biodiversity (Huvenne and Davies, 2013).

As our knowledge and understanding of the importance of submarine canyons for biodiversity has improved, our need for a systematic approach to describing and classifying them has grown. In this paper we review the geomorphological classification of canyons and relate specific geomorphic attributes to the physical oceanographic and ecological processes that have been identified by previous workers as being important to defining differences in canyon ecosystems (e.g., Schlacher et al., 2007; Cartes et al., 2010; McClain and Barry, 2010; Vetter et al., 2010; others detailed in Section 3). In this context, we present a new submarine canyon dataset for the Australian continental margin, derive physical properties for all canyons and use these measures to classify Australian canyons as a framework for examining their geomorphic and ecological characteristics.

2. Definitions and canyon types

Here we adopt the criteria for submarine canyons proposed by Shepard (1972, 1981) who recognised that canyons may have several origins and restricted his definition to "steep-walled, sinuous valleys with V-shaped cross sections, axes sloping outward as continuously as river-cut land canyons and relief comparable to even the largest of land canyons". This definition therefore excludes other seafloor valleys, including: delta-front troughs (located on the prograding slope of large deltas); fan valleys (the abyssal, seaward continuation of submarine canyons some of which are remarkably long; Skene and Piper, 2006; Bourget et al., 2008); slope gullies (incised into prograding slope sediments); fault valleys (structural-related, trough-shaped valleys,

* Corresponding author.
E-mail address: Zhi.Huang@ga.gov.au (Z. Huang).

http://dx.doi.org/10.1016/j.margeo.2014.07.007

generally with broad floors); shelf valleys (incised into the shelf by rivers during sea level low stands, generally less than 120 m deep); and glacial troughs incised into the continental shelf by glacial erosion during sea level low stands, generally U-shaped in profile and having a raised sill at their seaward terminus (Shepard, 1981).

Among the submarine canyons that fit Shepard's criteria, there are two broad types: (i) Shelf-incising canyons, with the largest extending landward as shelf valleys that have a direct connection to modern river systems. A sub-category of shelf-incising canyon, termed “headless canyons”, incise the shelf but do not extend across the shelf as shelf valleys nor do they connect to river systems (Greene et al., 1991); (ii) Blind (slope-confined) canyons that are confined to the continental slope with heads that terminate below the shelf break (also termed slope-sourced canyons; Brothers et al., 2013).

3. Hydrodynamic and ecological significance of canyons

The topography of submarine canyons can influence local upwelling and downwelling of water masses and generate other complex hydrodynamic processes, notably internal tides (Shepard, 1975; Hotchkiss and Wunsch, 1982; Klinck, 1996; Allen et al., 2001; Cacchione et al., 2002; Carter and Gregg, 2002). Canyons may also act as conduits for transporting sediment and nutrients from the shelf to the deep sea (Gardner, 1989a; Vetter and Dayton, 1998, 1999; Canals et al., 2006; de Stigter et al., 2007; Zuniga et al., 2009; Cunha et al., 2011; Martin et al., 2011; Puig et al., 2013). Internal tides and waves, in contrast, can resuspend sediments through focusing effects and transport them up-canyon and across the shelf break (Shepard et al., 1974a, 1974b; Gardner, 1989b; Kunze et al., 2002; de Stigter et al., 2007; Puig et al., 2013). The combined effects of these hydrodynamic processes enhance shelf-slope exchanges and vertical motions of water and materials (Allen et al., 2001; Jordi et al., 2005) and have a substantial influence on the physical and biochemical properties of submarine canyons.

Of particular importance to canyon ecology are enhanced nutrient levels (e.g. chlorophyll-a, organic carbon and nitrogen, lignin) in the water column and sediment (Palanques et al., 2005; Garcia et al., 2008; Zuniga et al., 2009; Tesi et al., 2010; Kiriakoulakis et al., 2011; Martin et al., 2011; van Oevelen et al., 2011; De Leo et al., 2012) and the vertical profiles of light availability (turbidity), temperature, salinity and oxygen (Bosley et al., 2004; S.J. Rennie et al., 2009; Zuniga et al., 2009; Martin et al., 2011; De Leo et al., 2012). Together with large depth ranges, steep walls, rocky outcrops and mixed sediment types, these factors contribute to high spatial and temporal heterogeneity of canyon habitats which may in turn facilitate high marine biodiversity (Schlacher et al., 2007; McClain and Barry, 2010).

Refuge and food supply are two determining factors of habitat quality. Submarine canyons commonly have heterogeneous substrate types that offer habitats for various benthic species (e.g., Vetter et al., 2010; Cunha et al., 2011; De Mol et al., 2011; Paterson et al., 2011). In addition, canyons can provide natural refuge from fishing activities (Yoklavich et al., 2000) and harbour relic species (Gili et al., 2000; Palanques et al., 2005). Increased food supply in the vicinity of canyon heads and the upper reaches of canyons can lead to strong primary and secondary production (Vetter, 1994; Skliris and Djenidi, 2006; Cartes et al., 2010; Vetter et al., 2010). The aggregation effect of the food web enhances species diversity (Gili et al., 2000; Genin, 2004; van Oevelen et al., 2011). Numerous studies have demonstrated the significant biodiversity values of submarine canyons for:

- benthic macrofauna such as polychaetes (e.g., Rowe et al., 1982; Vetter, 1994; Vetter and Dayton, 1998; Cartes et al., 2010; Louzao et al., 2010; Cunha et al., 2011; Paterson et al., 2011; Currie and Sorokin, 2014; De Leo et al., 2014);
- benthic megafauna such as sponges and cold-water corals (e.g., Rowe, 1971; Vetter and Dayton, 1999; Hargrave et al., 2004; Schlacher et al., 2007; Cartes et al., 2010; De Leo et al., 2010; Ramirez-Llodra et al., 2010; Vetter et al., 2010; De Mol et al., 2011);
- phytoplankton (e.g., Skliris and Djenidi, 2006; Mendes et al., 2011);
- zooplankton such as krill (e.g., Greene et al., 1988; Allen et al., 2001; Skliris and Djenidi, 2006; Robison et al., 2010);
- fish and invertebrates such as rockfish, Pacific ocean perch and giant squid (e.g., Vetter and Dayton, 1999; Yoklavich et al., 2000; Brodeur, 2001; De Leo et al., 2010; Vetter et al., 2010; Guerra et al., 2011; De Leo et al., 2012); and
- whales (e.g., Hooker et al., 1999; S. Rennie et al., 2009).

4. Submarine canyons in Australia

The distribution of submarine canyons on the Australian margin was first mapped at the national scale by Heap and Harris (2008). A total of 423 submarine canyons was identified on all margins of the continent, with the greatest number ($n = 127$) along the southeast margin where the continental shelf and slope are both relatively narrow and steep. In contrast, only seven canyons were identified on the broad shelf of the northern margin (Heap and Harris, 2008). This contrast in the distribution of canyons in relation to the shelf and slope of the Australian margin was further highlighted by Porter-Smith et al. (2012) in a morphometric analysis of 257 canyon catchments.

In addition to these continent-wide studies, Australian submarine canyons have been mapped at local to regional scales along the south-western (Von Der Borch, 1968; Exon et al., 2005), south-south-eastern (Hill et al., 1998; Gingele et al., 2004; Hill et al., 2005; Mitchell et al., 2007) and north-eastern (Puga-Bernabeu et al., 2011, 2013, 2014; Webster et al., 2012) margins with a focus on canyon geology, geomorphology and sedimentology. Canyon-specific studies of local patterns in benthic biodiversity (e.g. Schlacher et al., 2007; Currie et al., 2012; Currie and Sorokin, 2014) and of canyon oceanography (e.g. Perth Canyon; S. Rennie et al., 2009) have contributed to an improved understanding of canyons as sites of enhanced productivity. However, the drivers of broader regional patterns in biodiversity within and between canyons remain poorly understood.

Many canyons on the Australian margin are influenced to some degree by either the Leeuwin Current (western to southern margins) or the East Australian Current (eastern margin), in addition to more localised oceanographic phenomena such as the Ningaloo Current (central western margin), the Flinders Current (southern margin), and dense shelf water cascades such as documented for Bass Strait (Godfrey et al., 1980) and southwest Australia (Pattiaratchi et al., 2011). Many canyons are located within the new national network of Commonwealth Marine Reserves (CMRs) and are recognised as Key Ecological Features (KEFs) in the management plans for these reserves (Commonwealth of Australia, 2013a, b). In particular, it is the role that canyons play in channelling nutrient-rich waters and thereby promoting productivity that is highlighted in the profile descriptions of these canyon KEFs. It follows then that to support the management of these marine reserves and to better understand the ecological processes associated with submarine canyons, an integrated analysis of canyons and oceanography is required.

5. Data sources and methods

5.1. Bathymetry datasets

Our analysis covers the full extent of the Australian Exclusive Economic Zone (excluding the external territorial seas and extended continental shelf; Fig. 1), an area of 6.82 million km^2. The study area is arbitrarily divided into eight geographic regions, as defined by Heap and Harris (2008) (Fig. 1). The eight regions are used here to facilitate the presentation and comparison of the canyon mapping and classification results.

To map the submarine canyons on the Australian margin we used three bathymetry datasets. Dataset 1 is the national-scale bathymetry

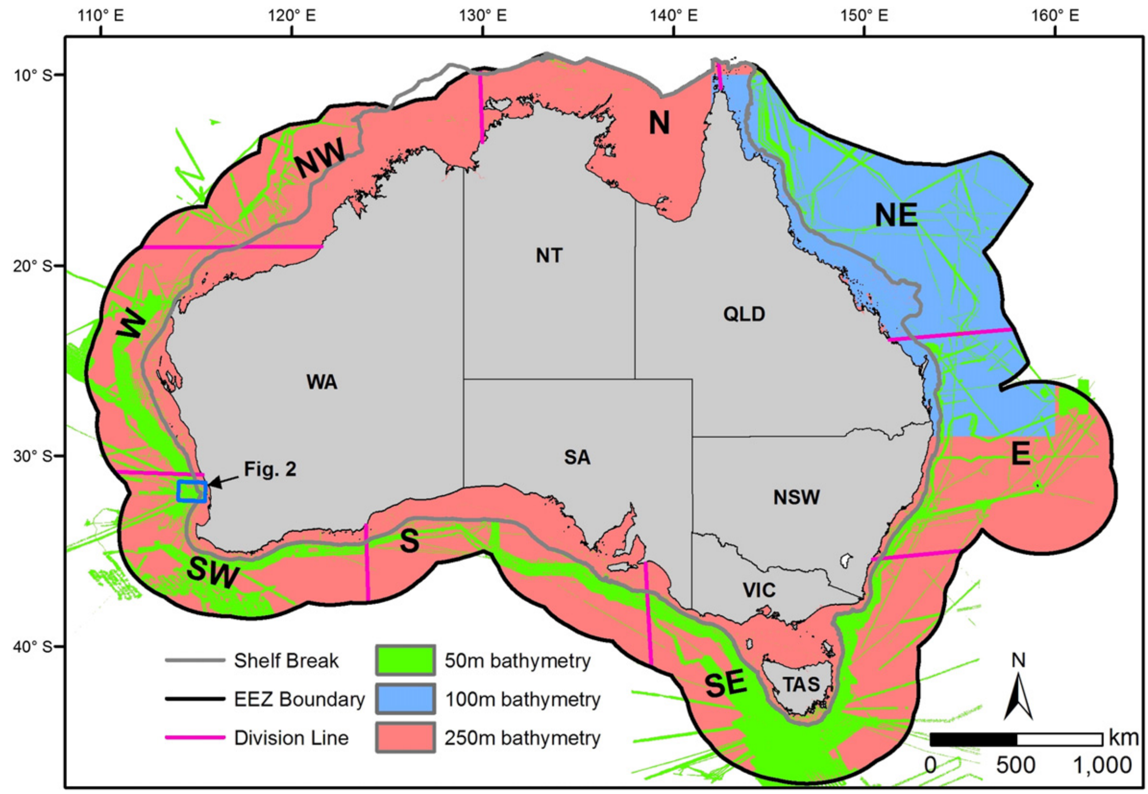

Fig. 1. The study area showing extents of bathymetry datasets used to map submarine canyons on the Australian margin. The eight geographic regions previously defined by Heap and Harris (2008) (N—north, NW—northwest, NE—northeast, E—east, SE—southeast, S—south, SW—southwest, W—west) and the extent of Fig. 2 are also shown.

grid that covers the entire study area (Fig. 1) with a spatial resolution of ~250 m (Whiteway, 2009). It is the latest update of the grid used by Heap and Harris (2008) to map the seabed geomorphic features on the Australian margin. The 250 m bathymetry grid was derived from multibeam and single beam data, Australian Hydrographic Service Laser Airborne Depth Sounding data, Royal Australian Navy fairsheets, the General Bathymetric Chart of the Oceans (GEBCO) bathymetric model, and the 1 and 2 arc minute ETOPO satellite derived bathymetry (Whiteway, 2009). Dataset 2 is an ~100 m resolution bathymetry grid covering the Great Barrier Reef and Coral Sea regions (Fig. 1) produced by Beaman (2010) using the latest data from multibeam and single beam surveys, airborne LIDAR surveys, and satellite remotely sensed imagery. Dataset 3 includes multibeam sonar data gridded to 50 m resolution and compiled as tiles that provide coverage for 1.11 million km^2 of the margin (Wilson, 2012; Fig. 1). Importantly, these higher resolution multibeam bathymetry data include large sections of the outer continental shelf to upper continental slope, where most Australian submarine canyons are located (Heap and Harris, 2008; Harris and Whiteway, 2011).

5.2. Mapping method

Submarine canyons are complex and heterogeneous seabed features with steep walls, relatively flat bottoms and variable shapes, often with multiple branches. It is therefore currently difficult to delineate canyon extents using automatic techniques such as GIS-based segmentation, which is designed to obtain relatively homogeneous spatial objects (features) ideally from continuous high resolution multibeam bathymetry data across each canyon. We therefore used a manual digitising method to map canyon boundaries, following Heap and Harris (2008). First, we generated hill-shaded layers from the bathymetry datasets to enhance the topography of seabed features and assist the identification of canyon catchment (drainage) boundaries (Porter-Smith et al., 2012). These boundaries were manually digitised as GIS polygons on the hill-shaded bathymetry layers. We also digitised one canyon head and foot for each canyon (non-branched and multi-branched canyons alike). As an example, Fig. 2 illustrates the resultant polygon, canyon head and foot, and centrelines (detailed below) for the multi-branched Perth Canyon.

After mapping all canyon-like features on the Australian margin, we applied the following filtering criteria to obtain the final set of canyon polygons: (i) the water depth at the canyon head is less than 4000 m; (ii) the incision of the canyon head relative to the surrounding interfluve is greater than 100 m (detailed further in Section 5.3), and (iii) the depth range between the canyon head and foot is greater than 600 m. These criteria follow the global canyon mapping study of Harris and Whiteway (2011), with the exception of the threshold for the depth range. In this continental scale study we considered the 600 m threshold as more appropriate (rather than 1000 m as used by Harris and Whiteway, 2011). Together, these criteria ensure the dataset excluded non-canyon features such as abyssal valleys, slope gullies and shallow shelf valleys.

The bathymetry datasets used for the submarine canyon mapping have different spatial resolutions and variable uncertainty levels. To address this data quality and uncertainty issue, we assigned each canyon an uncertainty score, largely based on the spatial resolution of the bathymetry datasets underlying the canyon. The uncertainty scores range from 1 to 5, to represent the least to the most uncertain mapping, respectively. Canyons with uncertainty scores of 1 and 2 were mapped almost exclusively using the multibeam bathymetry dataset with 50 m spatial resolution. The canyons that were mapped using a combination of the bathymetry datasets with higher and lower spatial resolutions were assigned uncertainty scores between 3 and 5.

5.3. Canyon metrics

For each canyon polygon, a total of 30 metrics (attributes) were derived based on its shape, morphometric characteristics and

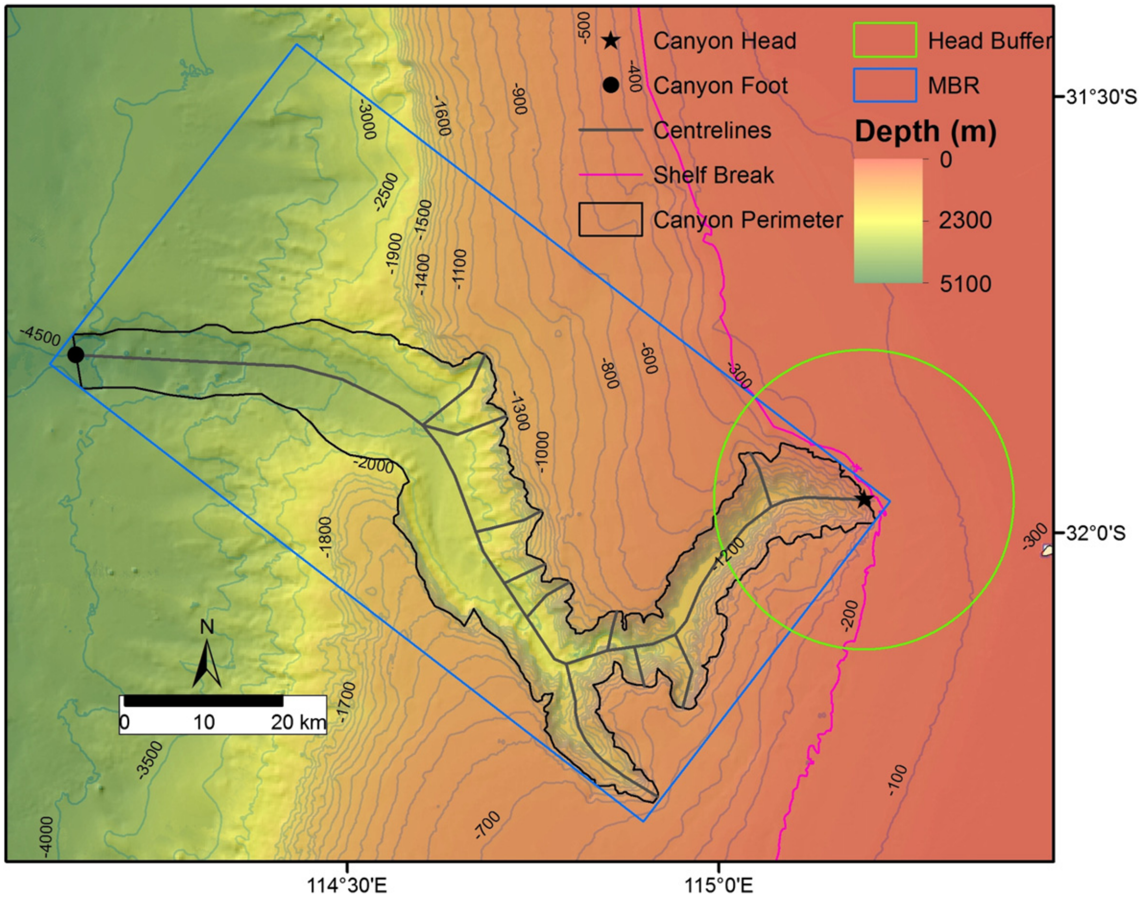

Fig. 2. Perth Canyon showing key parameters measured for all canyons in this study, including: Canyon Head depth (281 m); Canyon Foot depth (4683 m); Centreline distance for the main axis and tributaries (224 km); Canyon Perimeter (386 km); Maximum Bounding Rectangle (MBR; 51 × 95 km) and the Canyon Head Buffer. Additional derived parameters are listed in Table 1. Location of Perth Canyon is shown in Fig. 1.

geographical location (Table 1). Some of these metrics were calculated in ArcGIS Desktop™ and are self-explanatory, such as planar area (PA), perimeter (Pm) and depth range (DR). The methods to obtain and calculate other metrics were as follows:

- Centreline length (CL) is defined as the length of the "centreline" of an elongated canyon polygon (Fig. 2). In this study, the centreline was used as an approximate representation of the canyon thalweg. The centrelines were generated using the ArcScan toolset available in ArcGIS Desktop™. For a dendritic canyon, CL was calculated as the length of the main canyon plus all tributary canyon centrelines.
- Minimum bounding rectangle (Mbr) was defined as the minimum rectangle enclosing a canyon polygon (Freeman and Shapira, 1975; Toussaint, 1983; Fig. 2). The rectangle width (MbrW), length (MbrL) and orientation (degrees relative to north; MbrO) were calculated, as well as the length to width ratio (LtWR), the border index (BI) and compactness (Cp), using the following equations:

$$\mathrm{LtWR} = \frac{\mathrm{MbrL}}{\mathrm{MbrW}}; \tag{1}$$

$$\mathrm{BI} = \frac{\mathrm{Pm}}{(\mathrm{MbrL} + \mathrm{MbrW}) \times 2}; \tag{2}$$

$$\mathrm{Cp} = \frac{\mathrm{MbrW} \times \mathrm{MbrL}}{\mathrm{PA}}. \tag{3}$$

- Canyon volume (Vm) was defined as the 3-D space bounded by the canyon bottom and walls. It was calculated from the volumetric difference between a reference surface (in 3-D) and the canyon surface (in 3-D) using the "Surface Difference" tool in ArcGIS Desktop™. Both the canyon surface and reference surface are bathymetric surfaces; and the canyon surface is below the reference surface. The canyon surface was created by converting the canyon polygon to raster layer, then to a TIN surface. The reference surface is the surface over the top of the canyon walls, created by: (i) extracting depth values for all vertices along the canyon polygon, effectively representing the top of canyon walls; (ii) creating an interpolated raster layer based on these depths using the "TopoToRaster" tool in ArcGIS Desktop™; and (iii) converting the interpolated raster layer to a TIN as the reference surface.
- Sinuosity (Sn) was calculated using the following equation:

$$\mathrm{Sn} = \frac{\mathrm{CL}}{\mathrm{HtFD}} \tag{4}$$

where HtFD is the head to foot distance.

- Head incision (HI) depth was calculated as the depth range within a 2 km buffer around a canyon head (Fig. 2). This distance was chosen on the basis that most canyon heads exert maximum influence on

Table 1
Descriptions of canyon metrics.

Name	Code	Definition	Units	Group
Planar area	PA	Area of canyon polygon	km^2	Shape
Perimeter	Pm	Perimeter of canyon polygon	km	Shape
Centreline length	CL	Total length of canyon/sub-canyons centreline(s)	km	Shape
Minimum bounding rectangle width	MbrW	Width of the minimum rectangle that encloses the canyon polygon	km	Shape
Minimum bounding rectangle length	MbrL	Length of the minimum rectangle that encloses the canyon polygon	km	Shape
Minimum bounding rectangle orientation	MbrO	Orientation of the minimum rectangle that encloses the canyon polygon	Degrees[1]	Shape
Length to width ratio	LtWR	A measure of elongation. Larger the value the more elongate the canyon	None	Shape
Border Index	BI	A measure of geometric complexity. Larger the value the more fractal the canyon	None	Shape
Compactness	Cp	A measure of compactness. Larger the value the more compact the canyon (or the smaller its border)	None	Shape
Number of branches	NoB	Number of sub-canyons	Integer	Shape
Volume	Vm	3-D volume enclosed by the canyon bottom and walls	km^3	Shape
Head to foot distance	HtFD	Euclidian distance between canyon head and foot	km	Shape
Sinuosity	Sn	A measure of the quality of being sinuous. Larger the value the more sinuous the canyon	None	Shape
Head incision	HI	Incision depth of canyon head	m	Morphometric
Average gradient	AG	Average gradients within canyon polygon	Degrees	Morphometric
Standard deviation of gradient	StdG	Standard deviation of the slope gradients within canyon polygon	Degrees	Morphometric
Range of gradient	RG	Range between maximum and minimum gradients within canyon	Degrees	Morphometric
Surface area	SA	3-D surface area of canyon	km^2	Morphometric
Rugosity	Rg	Roughness of canyon surface	None	Morphometric
Head to foot gradient	HtFG	Gradient between canyon head and foot	Degrees	Morphometric
Percentage of gradient greater than 15°	pG15	Percentage of canyon area with slope gradients greater than 15°	%	Morphometric
Head depth	HD	Water depth of canyon head	m	Location
Foot depth	FD	Water depth of canyon foot	m	Location
Depth range	DR	Depth range between canyon head and foot	m	Location
Incision depth[2]	ID	Averaged depth of canyon area that incises into shelf break	m	Location
Incision area[2]	IA	Area of canyon area that incises into shelf break	km^2	Location
Distance to shelf break[3]	DtSB	Euclidian distance of canyon to shelf break	km	Location
Distance to river mouth[2]	DtRM	Euclidian distance of canyon to the mouth of the nearest permanent river	km	Location
Distance to nearest canyon	DtNC	Euclidian distance to the nearest canyon	km	Location
Focal variety	FV	Number of neighbouring canyons within a nominated proximity	Integer	Location

[1] Relative to north for major axis.
[2] For shelf-incised canyons only.
[3] For blind canyons only.

hydrodynamic and ecological processes within an area that extends on the order of several kilometres (not tens of km) from the rim (Allen et al., 2001; Carter and Gregg, 2002; S. Rennie et al., 2009).

- Surface area (SA) incorporates the three-dimensionality of the seabed and is always greater than the planar area. The algorithm of Jenness (2004) was used to calculate the surface area of each canyon cell (after converting the polygon to a raster with a 50 m spatial resolution); then all cells within a polygon were summed to derive SA.
- Rugosity (Rg) was calculated as:

$$Rg = \frac{SA}{PA}. \quad (5)$$

- Head to foot gradient (HtFG) represents the gradient between the canyon head and foot and was calculated as:

$$HtFG = \mathrm{atan}\left(\frac{DR}{HtFD}\right) \times 180 \div \pi. \quad (6)$$

- Incision area (IA) and incision depth (ID) are two metrics generated for shelf-incising canyons only, using the shelf break line as the baseline. In Australian continental margins, the shelf break was conventionally defined by the 200 m contour (Butler et al., 2001; Porter-Smith et al., 2012). In this study, the shelf break line was mapped from the 200 m depth contour in the 250 m bathymetry grid and modified to fit the shelf break more accurately using the 100 m and 50 m bathymetry grids with the aid of their hill-shaded layers (Fig. 1). A 2 km buffer was then created around the shelf break line and where a canyon polygon intersected the buffer, ID was calculated as the average depth of the intersected area. Because we considered the shelf break as a zone rather than a 1-D line and that 2 km was an appropriate buffering distance. Similarly, IA was the planar area of the intersected area.
- Focal variety (FV) indicates the canyon spatial density, or spacing, calculated here using the "Focal Variety" tool in ArcGIS Desktop™ with a circle neighbourhood of a 100 km radius (Harris and Whiteway, 2011).

5.3.1. Classification system and analytical techniques

A hierarchical classification system was used to classify the canyons based on the metrics derived for each canyon polygon. At the top level of the classification tree (i.e. Level 1 (L_1)), a two-category classification was imposed on each canyon as being shelf-incising or blind (slope-confined) using the 'distance to shelf-break' (DtSB) metric. Canyons with heads at least 500 m shoreward of the shelf break and coincident with a landward deflection of the shelf break were classified as shelf-incising. These criteria were to exclude those canyons that merely touch the shelf break line and those that do not incur a landward deflection. All canyons that do not satisfy the above criteria in the dataset were classed as blind canyons. Subsequent levels of the canyon classification were determined using knowledge-driven (supervised) and data-driven (unsupervised) classification techniques separately. Both knowledge-driven and data-driven classification techniques have been successfully used in habitat mapping and classification (e.g. Harris et al., 2008; Harris and Whiteway, 2009; Harris, 2011; Huang et al., 2011). Knowledge-driven techniques are able to utilise expert knowledge gained from a growing body of scientific observations and research. The resultant classes use descriptive terms that are easily understood by end users. The classification process, however, involves a degree of subjectivity. Data-driven techniques, on the other hand, are more objective and automatic. They, however, tend to be more sensitive to data errors. The resultant classes are also more difficult to interpret. This study employed both techniques to take full advantage of their relative merits.

Table 2
Statistics of canyon metrics, summarised by canyon type (the highlighted values were used for the knowledge-driven classifications).

					Canyon type							
	All canyons				Shelf–incised canyons				Blind canyons			
	Min	Max	Mean	s.d.[1]	Min	Max	Mean	s.d.	Min	Max	Mean	s.d.
Pm	6.2	1320	88.8	116.0	15.7	1320	146.1	192.5	6.2	1294	80.0	96.5
PA	1.0	4695	157.3	353.6	4.2	4695	332.3	691.0	1.0	2906	130.4	257.1
CL	2.7	738.4	46.7	65.3	6.6	727.6	80.8	109.2	2.7	738.4	41.4	53.8
MbrW	0.6	114.3	8.4	10.3	1.1	114.3	12.9	15.9	0.6	61.5	7.8	8.9
MbrL	2.7	215.2	26.7	24.8	5.8	215.2	38.2	38.7	2.7	173.0	24.9	21.3
MbrO	0.2	179.6	83.2	43.8	4.6	178.0	86.4	34.6	0.2	179.6	82.7	45.1
LtWR	1.0	25.7	4.5	2.9	1.0	18.0	4.3	2.9	1.0	25.7	4.5	2.9
BI	0.8	3.8	1.1	0.3	0.9	3.2	1.3	0.5	0.8	3.8	1.1	0.3
Cp	1.1	10.3	2.2	0.8	1.5	10.3	2.7	1.2	1.1	6.0	2.2	0.7
NoB	1.0	47.0	2.8	3.4	1.0	25.0	4.4	4.9	1.0	47.0	2.6	3.1
HI	3.0	1664	605.9	270.1	3.0	1023	421.2	229.6	102.0	1664	634.3	264.8
HD	−4000	−13.0	−1414	1067	−471.0	−13.0	−180.6	91.1	−4000	−49.0	−1604	1021
FD	−5537	−108	−3170	1267	−5073	−108.0	−2297	1295	−5537	−784.0	−3304	1209
DR	34.0	4922	1756	944.4	34.0	4922	2117	1270	601.0	4686	1701	872.2
AG	0.1	38.1	12.7	4.9	0.1	21.7	11.8	4.9	1.8	38.1	12.8	4.9
StdG	0.1	20.0	8.5	2.8	0.1	13.6	7.7	3.1	0.9	20.0	8.6	2.7
RG	0.6	88.7	58.9	17.2	0.6	88.4	55.9	22.0	6.8	88.7	59.4	16.3
SA	1.0	4925	172.6	375.9	4.3	4925	357.3	724.8	1.0	2974	144.2	277.4
Rg	1.0	2.1	1.1	0.1	1.0	1.3	1.1	0.1	1.0	2.1	1.1	0.1
Vm	0.0	1346	20.1	71.3	0.0	1346	46.1	158.0	0.0	473.9	16.2	44.0
HtFD	2.6	203.7	26.1	24.0	5.7	203.7	37.5	37.6	2.6	169.0	24.3	20.7
HtFG	0.0	22.9	5.4	3.1	0.0	11.7	4.8	2.4	0.2	22.9	5.5	3.1
DtSB									0.0	757.3	65.3	104.9
DtNC	0.0	377.0	5.6	21.0	0.1	20.1	2.8	3.4	0.0	377.0	6.0	22.5
FV	1.0	46.0	19.2	9.9	4.0	46.0	20.9	10.2	1.0	46.0	18.9	9.8
ID					−798	−90.6	−410.5	156.1				
IA					1.6	3051	120.3	455.5				
pG15	0.0	96.4	32.7	19.8	0.0	75.4	30.3	19.4	0.0	96.4	33.0	19.9
Sn	1.0	7.7	1.6	0.9	1.0	7.7	2.0	1.3	1.0	7.4	1.6	0.8
DtRM	23.5	1136	221.7	211.6	23.5	456.2	90.8	83.7				

The knowledge-driven technique used in this study was based on the potential significance of the metrics outlined above in determining the nature of canyon habitats. From the 30 metrics calculated for all canyons, five metrics were selected as those that were most likely to be of ecological significance, as follows:

(i) The percentage of the canyon surface area having a slope gradient greater than 15° (pG15). This threshold value (15°) was chosen as the divide between hard (>15°) and soft (or unconsolidated) substrate (<15°), with the former a potential habitat for sessile organisms and associated faunas;
(ii) The head-to-foot gradient of the canyon (HtFG), a parameter that may influence slope stability and down-canyon sediment transport;
(iii) Canyon volume (Vm), a parameter that incorporates the surface area and depth of a canyon, and therefore, is a measure of the potential for a canyon to provide heterogeneous habitats;
(iv) Head incision depth (HI), which provides a measure of the bathymetric range at the canyon head and therefore the potential for exposed, hard substrate and for enhanced vertical mixing associated with upwelling and interaction with ocean boundary currents;
(v) Distance to the nearest canyon (DtNC), a parameter that indicates the degree of canyon clustering (or isolation) in a given area and in turn the potential for connectivity between more locally variable (or unique) habitats.

Other metrics may also be suitable for the knowledge-driven classification. For example, the Rugosity (Rg) metric, which indicates the roughness of canyon surface, can be used to replace the head-to-foot

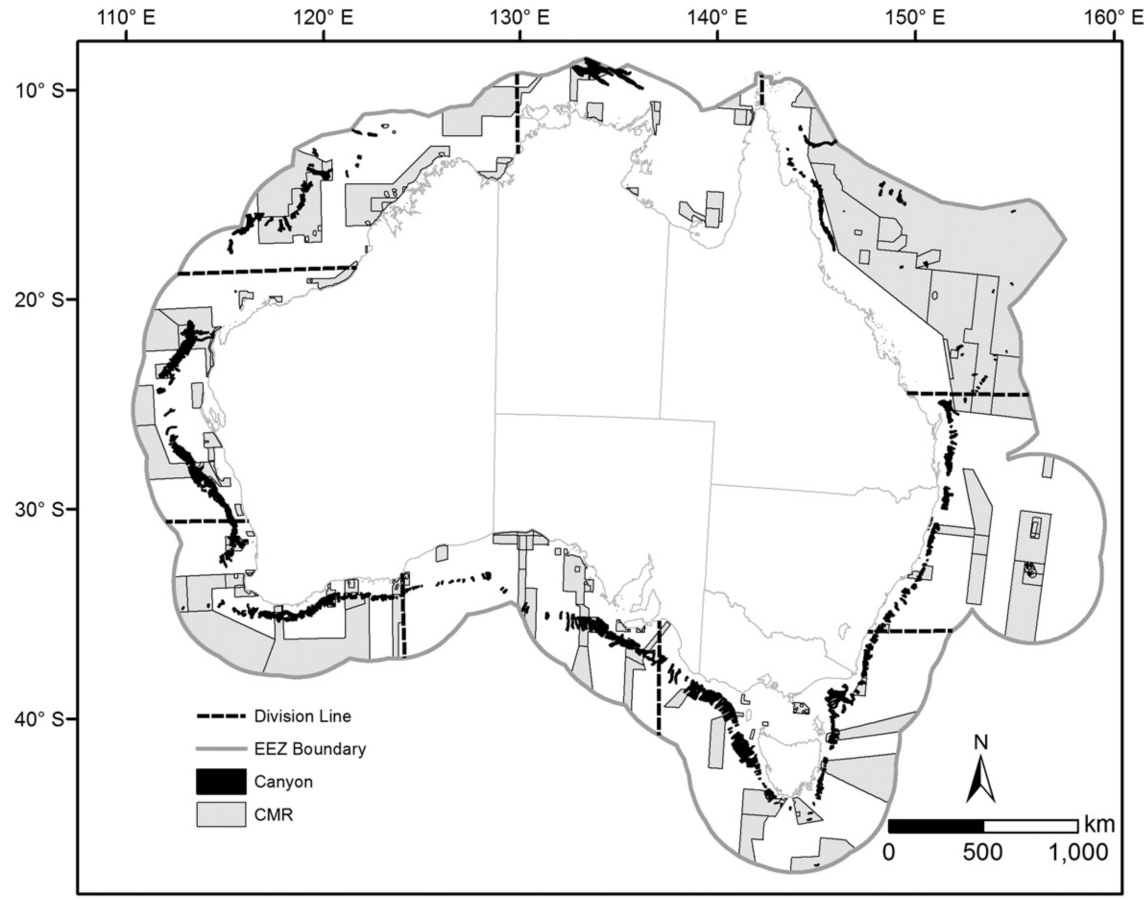

Fig. 3. Spatial distribution of the 713 mapped submarine canyons on the Australian margin, showing also the network of Commonwealth Marine Reserves (CMRs).

gradient or the proportion steeper than 15°. These five selected metrics were used to divide shelf-incising and blind canyons separately into sub-types across three further levels of classification (L_2, L_3 and L_4). These levels incorporated the gradient metrics (pG15 and HtFG for L_2), volume and depth metrics (Vm and HI for L_3) and spacing metric (DtNC for L_4) as a way of systematically assigning each canyon to a hierarchy of classes. The global mean values for these metrics were used as the class boundaries (the highlighted values in Table 2).

The data-driven classification employed an Expectation-Maximization (EM) clustering algorithm (Dempster et al., 1977) to derive three independent L_2 classifications based on canyon shape, morphometrics and geographical location. After taking into account the correlations among the canyon metrics, four metrics were selected for each classification. The shape-based classification used LtWR, Cp, BI and Vm. The morphometric-based classification used HI, pG15, HtFG and Rg. The location-based classification used HD, DR, DtNC, and either DtRM (for shelf-incising canyons) or DtSB (for blind canyons). For the EM algorithm, we set the maximum number of iterations to 100, then employed Akaike's Information Criterion (AIC; Akaike, 1974) and a five-fold cross-validation procedure to find the optimal number of clusters between 1 and 10. To verify whether the selected individual metrics are significant in separating the resultant clusters, an analysis of variance (ANOVA) using the F-test was carried out and evaluated at 99% significant level. In other words, the result of the one-way ANOVA indicates whether the mean of the metric is different among the clusters. It should be noted that we use the terminology of "cluster" (instead of "class") for the results of the data-driven classification because a cluster does not have a meaningful class name associated with it.

Table 3
The areas (i.e. PA in Table 1) and numbers of submarine canyons in eight geographic regions, summarised for all canyons, shelf-incised canyons and blind canyons.

		NE	E	SE	S	SW	W	NW	N	Sum
All canyons	Area (km^2)	5274	10,271	25,995	14,140	15,890	19,506	11,138	9940	112,154
	Area (km^2)[1]	5720	4500	37,820	16,910	12,490	10,130	6020	10,560	104,150
	Number	109	88	187	69	101	110	43	6	713
	Number[1]	66	32	127	39	64	39	31	7	405
Shelf-incised canyons	Area (km^2)	600	3775	9147	2493	5607	7	0	9940	31,569
	Number	7	20	50	2	9	1	0	6	95
Blind canyons	Area (km^2)	4674	6496	16,848	11,647	10,283	19,499	11,138	0	80,585
	Number	102	68	137	67	92	109	43	0	618

[1] The numbers were extracted from Heap and Harris (2008).

Table 4
Uncertainty levels of the Australian submarine canyons.

Uncertainty Score	All canyons	Shelf-incised canyons	Blind canyons
1	59 (8.3%)	27 (28.4%)	32 (5.2%)
2	243 (34.1%)	52 (54.7%)	191 (30.9%)
3	258 (36.2%)	10 (10.5%)	248 (40.1%)
4	106 (14.9%)	0 (0.0%)	106 (17.2%)
5	47 (6.6%)	6 (6.3%)	41 (6.6%)

6. Results

6.1. Canyon distribution and form

In total, 713 submarine canyons were identified and mapped on the Australian margin (Fig. 3). This includes all canyons that satisfied the criteria we used to filter out non-canyon-like features such as valleys and gullies, and six canyon-like features in the Arafura Sea (the northern region) that are located entirely on the continental shelf. While these six canyon-like-features fail the criteria in terms of their depth range, they are potentially important to the ecosystem processes on the northern shelf and are recognised as Key Ecological Features for the North Marine Region (Commonwealth of Australia, 2013b) (Fig. 3). This new tally of 713 canyons is a substantial increase on the 405 mapped by Heap and Harris (2008) (the tally of 405 excluded canyons they identified in the external territorial seas and extended continental shelf, Table 3) and the 256 mapped by Harris and Whiteway (2011). These previous efforts at mapping Australian submarine canyons each used lower resolution bathymetry datasets (250 m and 2 km, respectively).

In terms of the uncertainty score applied to each canyon, 42% of the 713 canyons was mapped from the high-quality multibeam bathymetry dataset and assigned scores of 1 and 2 (Table 4). A further 36% has an acceptable uncertainty score of 3 and the remaining 22% a score of 4 or 5. The submarine canyons identified here occupy a total area of 112,154 km^2, which is 1.64% of the continental EEZ and 8004 km^2 greater than the area reported by Heap and Harris (2008). With reference to the eight geographic regions of the Australian continent used by Heap and Harris (2008; Fig. 1), the southeast region has the greatest number of canyons while the northern region has the fewest (Table 3). Half of the canyons are located on the southern margin (SE, S and SW regions). On average, canyons in the northeast region are the smallest in area while canyons on the western margin are larger than those on the eastern margin.

6.2. Geomorphology of Australian submarine canyons

Submarine canyons on the Australian margin are highly variable in size, with planar areas ranging from 1 km^2 to 4695 km^2 (mean: 157 km^2; standard deviation: 353 km^2) and volumes of <0.01 km^3 to 1346 km^3 (mean: 20 km^3; standard deviation: 71 km^3) (Fig. 4 and Table 2). The planar shape of these canyons is also diverse. Most are elongate (83% with LtWR > 2.0, mean LtWR = 4.5), many are more or less fractal (47% with BI > 1.0, mean BI = 1.1), the majority are compact (89% with Cp > 1.5, mean Cp = 2.2), and many are dendritic (53% with NoB > 1, mean NoB = 2.8) (Fig. 4 and Table 2). On average, canyon heads incise more than 600 m into the seabed. Average gradients on canyon walls are ~13° with an average 33% of canyon area steeper than 15° (pG15) (Table 2). Average head to foot gradients (HtFG) are ~5.4° (Table 2).

Canyons on the Australian margin vary in extent across the outer continental shelf and continental slope to abyssal plain, with the shallowest canyon head in 13 m water depth (offshore the Great Barrier Reef) and the deepest head at 4000 m (on the northwest margin), with an average total depth range (DR) of 1756 m (Table 2). Most canyons are well separated from the coast and river mouths, with the closest canyon 23.5 km from a permanent river mouth and the farthest 1136 km away (mean: 221 km) (Table 2). The majority of canyons are closely spaced in clusters, with mean spacing of 5.6 km (Table 2). Within a neighbourhood radius of 100 km there are, on average, 19 canyons (Table 2).

6.3. Canyon classification

6.3.1. Shelf-incising and slope-confined (blind) canyons

Among the 713 mapped canyons, 95 are classified as shelf-incising and 618 as slope-confined (or blind) canyons. Shelf-incising canyons are generally larger, ranging in area from 4.2 to 4695 km^2 (mean: 332 km^2), and collectively cover 28% of the mapped canyon area (Table 2). Shelf-incising canyons also have different geometric (shape), morphometric and location characteristics to blind canyons (Table 2 and Fig. 4). On average, shelf-incising canyons are less elongate, more fractal, more compact, more sinuous and more dendritic. These canyons have less complex seabed topography but are shallower, span a greater water depth range and more closely spaced. Table 3 and Fig. 5 show the distribution of shelf-incising and blind canyons among the eight geographic regions. More than half of the shelf-incising canyons are located in the southeast region, including the large, dendritic Bass Canyon system comprised of six tributary canyons: Everard, Anemone, Archer, Pisces, Moray and Mudskipper Canyons (Fig. 5h; Mitchell et al., 2007). The region also contains The Ling Hole Canyon, Pieman Canyon, Southwest Cape Canyon, Riedle Canyon and King Island Canyon. A further 20% of the shelf-incising canyons is in the east region, including Long Nose Canyon (Fig. 5e). The southwest region has nine shelf-incising canyons, including Perth Canyon, Pallinup Canyon, Mermaid Canyon, Kalgan Canyon, Denmark Canyon, Wilson Canyon and Bremer Canyon (Fig. 5f). The northeast region has seven unnamed, shelf-incising canyons (Fig. 5c). The North region has six canyons in the Arafura Sea (Fig. 5b). The southern region has two shelf-incising canyons, Sprigg Canyon and Du Couedic Canyon (Fig. 5g). The west region has one unnamed shelf-incising canyon and the northwest region has no shelf-incising canyons (Fig. 5a, d). Blind canyons are absent from the northern region, but are otherwise relatively evenly distributed among the other seven geographic regions.

6.3.2. Knowledge-driven classification

For both shelf-incising and blind canyons, using the global mean values highlighted in Table 2, the knowledge-driven classifications yielded four classes at L_2: "steep wall, steep gradient"; "steep wall, gentle gradient", "gentle wall, steep gradient", and "gentle wall, gentle gradient". At L_3 a further four classes were obtained: "large volume with large head incision", "large volume with small head incision", "small volume with large head incision", and "small volume with small head incision". Finally, at L_4 the two resultant classes are "widely spaced" and "adjacent". For shelf-incising canyons, a class was further split only if there were more than 20 canyons in the class. This resulted in 10 classes (classification tree nodes; Fig. 6). For blind canyons, the splitting threshold was 35 canyons, which resulted in 22 classes (Fig. 7). The splitting thresholds were chosen to reduce the number of small final classes.

Among the 95 shelf-incising canyons, 43 are classed as gently sloping (i.e., "gentle wall, gentle gradient") with overall gradients less than 5.4° and less than 33% of their canyon walls steeper than 15° (Fig. 6). Of these, 37 have a volume less than 20 km^3 and a head incision less than 606 m (i.e., "small volume with small head incision"; L_3). Within this class, 31 are within 5.6 km of another canyon (i.e., "adjacent"). In sum, these are low gradient, relatively small, shallow and clustered canyons. An example of this relatively common type of shelf-incising canyon is Southwest Cape Canyon located off southern Tasmania (Fig. 8a). Much rarer are low gradient, shelf-incising canyons that are larger than 20 km^3, with Bass Canyon on the south-eastern margin and an unnamed canyon on the eastern margin as examples (Fig. 8b, c).

The second-most common class of shelf-incising canyon (n = 26) at L_2 is steeply sloping (>5.4° and >33% of canyon wall steeper than 15°) but varies in volume and head incision dimensions, resulting in four classes at level 3 of the hierarchy (Fig. 6). One of these classes comprises five canyons that have a large volume and large head incision depth (>20 km^3 and >606 m, respectively), four of which are located off the north coast of New South Wales and one off the northern Great Barrier Reef (Fig. 9). These particular canyons are all dendritic (8–10 branches, Table 5), with multiple gullies and steep canyon walls. As such, they are among the most topographically complex shelf-incising canyons on the Australian margin. In addition, they are also less elongate, less compact, more fractal, more closely spaced and closer to river mouths than the average shelf-incising canyon (Tables 2, 5). Examples of the other three L_3 classes under the "steep wall, steep gradient" category, defined by canyon volume and head incision depth, include an unnamed canyon that incises the Great Barrier Reef shelf, Sprigg Canyon and Riedle Canyon (Fig. 8f, g, h).

The remaining 26 shelf-incising canyons can be divided into two L_2 groups. One group is composed of 15 canyons that are low gradient (<5.4°) but with relatively steep walls, an example of which is Bremer Canyon on the southern margin (Fig. 8e). The other group includes 11 canyons that have a steep gradient with relatively gentle walls, an example of which is Coral Canyon in Bass Strait (Fig. 8d). Neither of these two groups could be sub-divided any further by this analysis. In terms of the regional variability for shelf-incising canyons, the east and northeast regions are dominated by the "steep wall, steep gradient" canyons (Fig. 5c, e); the southwest region is dominated by the "steep wall, gentle gradient" canyons (Fig. 5f); while, the southeast region has a large number of the "gentle wall, gentle gradient" canyons (Fig. 5h); the "gentle wall, steep gradient" canyons are also predominantly located in the southeast region (10 out of 11; Fig. 5).

Of the 618 blind canyons, almost half (n = 275) are gently sloping with overall gradients less than 5.4° and less than 33% of their canyon walls steeper than 15° (Fig. 7). Approximately one-third (n = 208) is steep, with a head to foot gradient greater than 5.4° and more than 33% of their canyon walls is steeper than 15°. The remaining 135 blind canyons are either gentle in overall gradient with steep walls (n = 79) or steep in overall gradient with gentle walls (n = 56). At the next level of the hierarchy (L_3), these four classes divide into 16 sub-classes based on canyon volume and depth of head incision. Of these, most blind canyons fall into two groups: small volume (<20 km^3) low gradient canyons with head incision less than 606 m (n = 156), and; small volume, steep canyons with head incision greater than 606 m (n = 142). The remaining 14 sub-classes at this level of the hierarchy have memberships in the range of 2 to 61 canyons and represent the full range of combinations of low/high overall gradient, gentle/steep walls, small/large volume and small/large head incision depth (Fig. 7).

The final level of the hierarchy (L_4) captures the strong degree of clustering among the more common types of blind canyons. Thus, 126 of the 142 small, steep canyons are located within 5.4 km of another canyon, and 125 of the 156 small, low gradient canyons are similarly proximal to another canyon. Many of these closely spaced blind canyons are along the western, south-western, and southern margins of the continent (Fig. 5). In terms of the regional variability for blind canyons, the east region is dominated by the "steep wall, steep gradient" canyons (Fig. 5e); the west region is dominated by the "gentle wall, gentle gradient" canyons (Fig. 5d); the southwest and southeast regions have larger percentages of the "steep wall, steep gradient" and "gentle wall, gentle gradient" canyons (Fig. 5f, h); the south region has more "steep wall, steep gradient" canyons than other classes (Fig. 5g); the northwest region is dominated by the "gentle wall, gentle gradient" canyons (Fig. 5a); while, the northeast region has more "gentle wall, gentle gradient" canyons than other classes (Fig. 5c).

6.3.3. Data-driven EM classification

For shelf-incising canyons, the EM algorithm resulted in two clusters based on the shape metrics, two clusters based on morphometrics and three clusters based on location metrics (Fig. 10). Of the four shape metrics, three were significant in separating the two clusters; the length-to-width ratio, border index and canyon volume (Table 6). Generally, the canyons in cluster 2 (n = 64) are more elongate, less fractal and much smaller in volume than the cluster 1 (n = 31) canyons (Fig. 10). Most of these canyons are located in the southeast region (Fig. 5h). For the morphometric-based clusters, all four metrics were significant in separating the two resulting clusters; namely, head incision depth, percentage of gradient greater than 15°, canyon head-to-foot gradient and rugosity (Table 6). In this result, the canyons in cluster 2 (n = 46) are more complex in seabed topography, with greater head incision depths, greater head-to-foot gradients, larger percentage of steep walls, and higher rugosities (Fig. 10). The east, southeast, southwest and northeast regions have a good number of these canyons, whereas canyons in cluster 1 are predominantly in the southeast region (Fig. 5).

The location-based clustering indicates that three metrics are significantly different among the three clusters; canyon head depth, depth range and distance to the nearest canyon (Table 6 and Fig. 10). The canyons in cluster 2 (n = 51) have the shallowest canyon head depths and smallest depth range, while canyons in cluster 1 (n = 34) have a greater depth range and are closely spaced whereas the canyons in cluster 3 (n = 10) have the deepest canyon heads and are most widely spaced. Most of the cluster 2 canyons are in the southeast region, whereas the southeast and east regions have more cluster 1 canyons and the canyons in cluster 3 are mostly located in the east region (Fig. 5).

For the blind canyons, the EM algorithm resulted in four clusters based on shape metrics, five clusters based on the morphometrics and four clusters based on location metrics (Fig. 11). All of the four shape metrics were significant in separating the four resulting clusters, including the length to width ratio, border index, compactness and canyon volume (Table 6). In general, these clusters (n = 78, 79, 228, 233, respectively) define a trend of increasing elongation and decreasing volume between clusters 1 and 4 (Fig. 11). In addition, cluster 2 is the most fractal and compact. Most of the regions are dominated by canyons in cluster 3 and cluster 4 (Fig. 5). Canyons in cluster 1 are roughly distributed across all regions except the northeast; while, two-thirds of canyons in cluster 2 is located on the west, southeast and northeast regions (Fig. 5). All morphometrics were also significant in separating the five resulting clusters (n = 33, 103, 225, 88, 169, respectively) (Table 6). Overall, canyons in cluster 1 have the most complex topography (Fig. 11). Most of them are located on the southeast, southwest and south regions (Fig. 5). Canyons in cluster 3 are clearly the least complex in topography. About two-thirds of them is located on the west and southeast regions.

Fig. 4 Boxplots of canyon metrics for all mapped canyons (All), shelf-incising canyons (SIC) and blind canyons (BC), including: (a) Perimeter area; (b) Perimeter; (c) Centreline length; (d) Minimum bounding rectangle width; (e) Minimum bounding rectangle length; (f) Minimum bounding rectangle orientation; (g) Length to width ratio; (h) Border index; (i) Compactness; (j) Number of branches; (k) Volume; (l) Head to foot distance; (m) Sinuosity; (n) Head incision depth; (o) Average gradient; (p) Standard deviation of gradient; (q) Range of gradient; (r) Surface area; (s) Rugosity; (t) Head to foot gradient; (u) Percentage of gradient greater than 15°; (v) Head depth; (w) Foot depth; (x) Depth range; (y) Incision depth; (z) Incision area; (aa) Distance to shelf break; (ab) Distance to river mouth; (ac) Distance to nearest canyon; (ad) Focal variety index. The thick line in the middle of each box is the median value for each parameter, with the 25th and 75th percentiles represented at the top and bottom of each box, respectively. The range of data is represented by the whiskers (dotted lines) outside the boxes. Circles represent outliers that are more than 1.5 times the interquartile range.

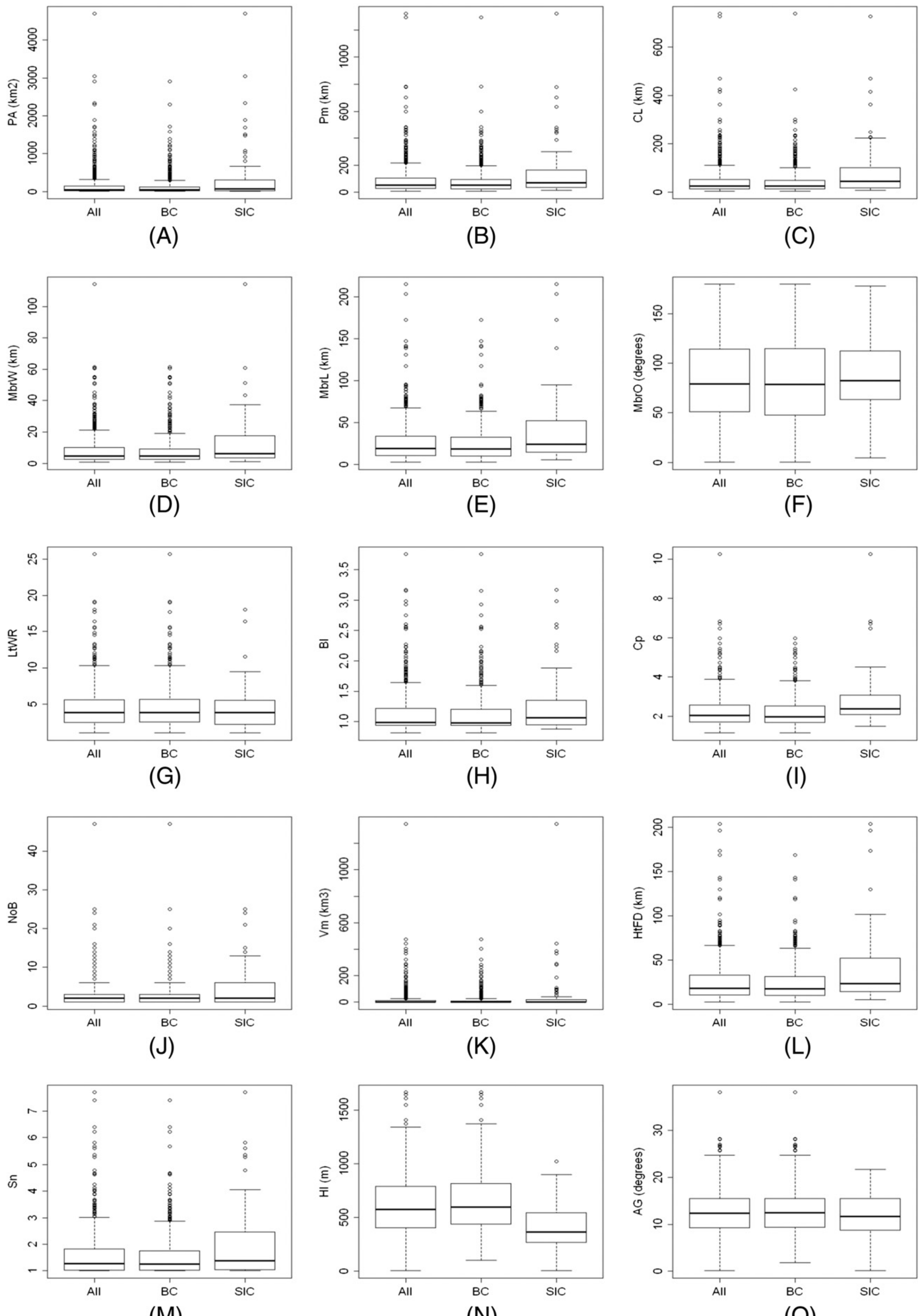

PA (km2)
All
BC
SIC
(A)
Pm (km)
(B)
CL (km)
(C)
MbrW (km)
(D)
MbrL (km)
(E)
MbrO (degrees)
(F)
LtWR
(G)
BI
(H)
Cp
(I)
NoB
(J)
Vm (km3)
(K)
HtFD (km)
(L)
Sn
(M)
HI (m)
(N)
AG (degrees)
(O)

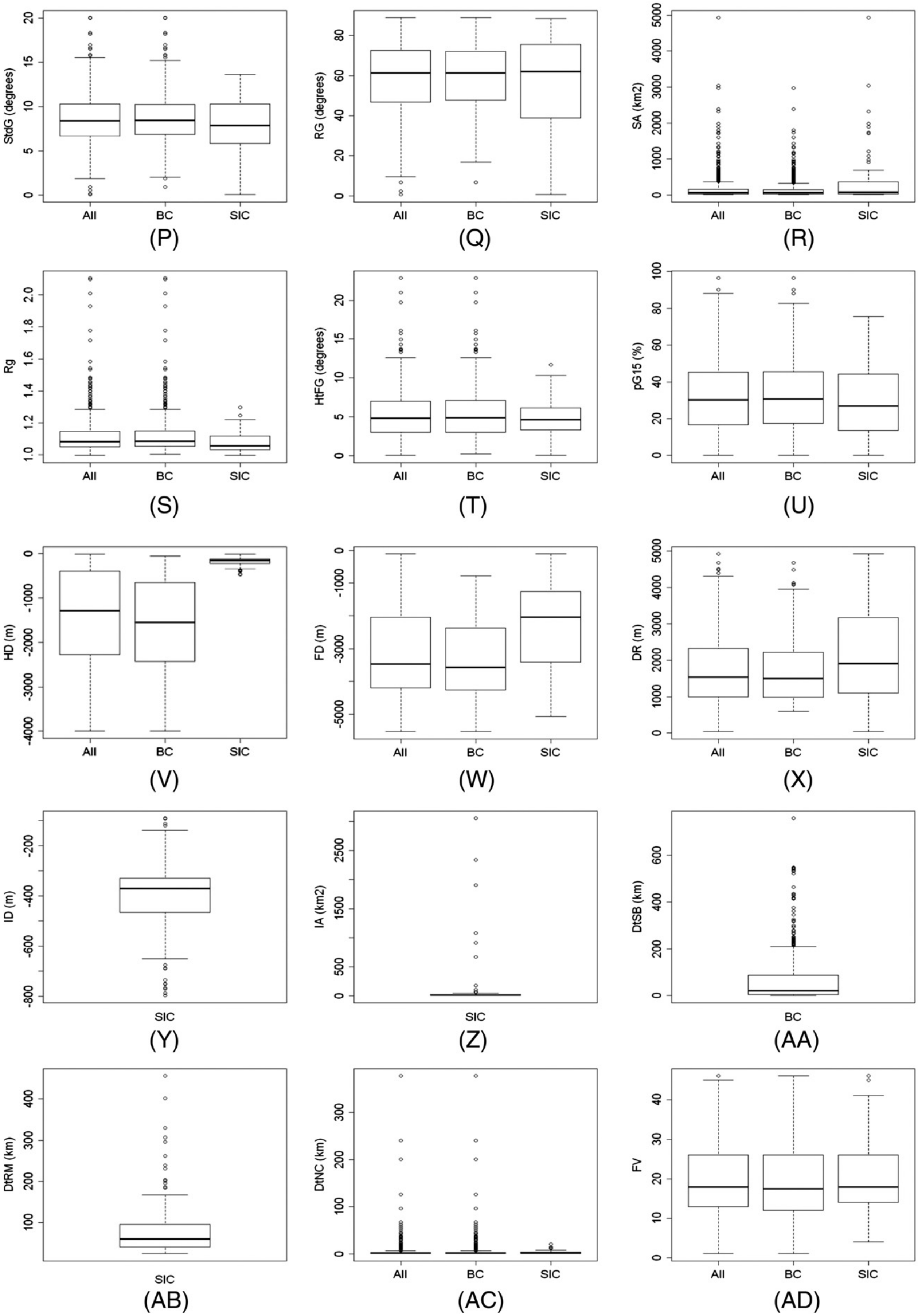

Fig. 4 (*continued*).

For the clusters defined by location metrics, all four variables were significant (Table 6). Canyons in cluster 1 (n = 241) have the largest depth range and exhibit the closest spacing (Fig. 11). Most of them are located in the southwest, southeast, east and south regions (Fig. 5). Canyons in cluster 2 (n = 184) that have the deepest canyon heads are located mostly in the west region, which has the largest number of these canyons (n = 81; Fig. 5). Canyons in cluster 3 (n = 110) have the shallowest canyon head depths, the smallest depth range, are closest to the shelf break and have the second closest spacing. Most of them are located in the southeast and northeast regions (Fig. 5). Canyons in cluster 4 (n = 83) are the farthest away from their neighbours and from the shelf break. Most of these canyons are located in the northeast region (n = 35; Fig. 5).

7. Discussion

7.1. Controls on the distribution and form of submarine canyons

The distribution and morphology of submarine canyons on the Australian margin reflect the plate tectonic history of the continent since the break-up of Gondwana and long-term processes associated with canyon development that vary at regional to local scales. This geological and process framework has been examined for some regions of the margin, providing context for discussing the distribution of canyon types documented in this study. These regions include the canyons in the Albany Group on the southwest margin (Exon et al., 2005; Fig. 5f), the Murray Canyons in the south (Fig. 5g) and Gippsland Canyons (including the Bass Canyon system) in the southeast (Fig. 5h) (Hill et al., 1998, 2005; Gingele et al., 2004; Mitchell et al., 2007) and the canyons that fringe the outer Great Barrier Reef (Puga-Bernabeu et al., 2011, 2013, 2014; Webster et al., 2012; Fig. 5c). These studies present detailed interpretations of seismic, bathymetric and sample (core) data that present evidence that canyons on these margins are ancient structures that were initiated as part of crustal subsidence associated with the opening up of the Southern Ocean, Tasman Sea and Coral Sea since the Late Cretaceous (Hill et al., 1998; Exon et al., 2005). Canyons on the west and northwest margins (Fig. 5a, d) have not been studied as extensively, but sampling of outcrop exposed in canyons on the west margin (Daniell et al., 2010) indicates that those canyons have also incised into Early Cretaceous sedimentary rocks that pre-date the break-up from the sub-continent of Greater India (Ali and Aitchison, 2005).

In several regions there is clear evidence for structural control of canyon form. For example, canyons in the Albany Group, the Murray Group and the Bass Canyon system incise the slope at oblique angles, display meandering form and/or have multiple tributaries that change direction abruptly and have been shown to be controlled by faults in basement rocks (Hill et al., 1998, 2005; Exon et al., 2005). For all these cases, the canyon morphology is complex with a dendritic plan form, large volume, steep gradient and often with deeply incised headwalls cut into soft sedimentary rocks. In the data-driven EM classification, eight complex shelf-incising canyons in the Albany Group are assigned to cluster 2 using four morphometric variables that describe complex topography (i.e. large head incision depth, steep head-to-foot gradient, high rugosity and high percentage of gradient greater than 15°; Figs. 5f; 10e–h). A similar result is found for the Murray Canyons (Fig. 5g).

In contrast to topographically complex canyons, many of which are shelf-incising, large numbers of closely spaced slope-confined canyons are simple in form with single valleys that run straight down the continental slope. This is particularly the case for slope-confined canyons on the western margin (Fig. 5d) and along the southern margin (western Murray Canyons; Fig. 5g). This characteristic morphology is interpreted to be a function of canyon incision into relatively uniform (soft) lithology of a thickly sedimented slope, with headward retreat the main mechanism of canyon evolution (Hill et al., 2005). For the western margin, the data-driven EM classification has assigned 83 slope-confined canyons to a cluster (C3) using morphometric metrics that describe canyons with small head incision depths, gentle head to foot gradients, low percentage of slope gradient greater than 15° and low rugosity (Figs. 5d; 11e–h). Further, the location based metrics for the western region assign 81 of the same canyons to a cluster (C2) that describes closely spaced canyons with canyon heads in deep water (2000–3000 m) located up to 100 km seaward of the shelf break (Fig. 11i, k, l). Based on these examples, we conclude that the classification results yield valuable insights into regional patterns in canyon form that can be linked to fundamental geological controls and related processes.

7.2. Modes of canyon evolution

Following the general model of canyon evolution proposed by Farre et al. (1983), submarine canyons on the Australian margin are considered to have evolved through a combination of mass wasting (gradual slumping, landslide events) and incision by erosive turbidity flows along pathways of least resistance, but with regional variability in the relative importance of each. In particular, regional to local differences in the supply of fluvial and shelf sediment to turbidity flows, and the width and gradient of the margin appear to have strongly influenced canyon development around Australia. These are discussed further below and related to the classification results from this study.

The supply of fluvial sediment to the Australian margin is low, with the continent yielding an estimated 46 t km^2 per year under the present-day arid climate; an order of magnitude less than Asia (244 t km^2 yr^{-1}) and only about four times greater than Antarctica (10 t km^2 yr^{-1}) (Ludwig and Probst, 1998). The Murray River is the primary source, delivering approximately half of the continent's sediment yield to the southern coast (25 t km^2 yr^{-1}). However, at present sea level very little (if any) of this sediment is transported across the shelf with the only terrestrial Holocene sediment in cores taken by Gingele et al. (2004) in the Murray Canyons limited to aeolian dust. In contrast, those same cores record high rates (up to 60 cm ka^{-1}) of fluvial sediment input into the Murray Canyons during sea-level lowstands of the Late Pleistocene. This sediment would have contributed to canyon incision directly by augmenting turbidity flows and indirectly by prograding the upper slope to shelf edge to the point of failure by slumping (Hill et al., 2005). Similar evidence for direct connections between rivers and canyons during Quaternary sea level lowstands is documented for the southeast (Gippsland canyons; Mitchell et al., 2007) and northeast regions (Webster et al., 2012). Overall, however, these are localised cases that contribute to the development of only a few shelf-incising canyons and are here represented in the data-driven EM scheme by canyons with high headwalls, steep gradients and high rugosity (e.g. Sprigg Canyon and Du Couedic Canyon in the Murray group that define morphometric cluster 2; Figs. 5g, 10e–h).

The great majority of submarine canyons on the Australian margin (including shelf-incising canyons) are disconnected from Quaternary river systems and have evolved by up-slope headwall retreat and incision by turbidity flows. Thus, canyons occur in greater density where the continental slope is steepest notably along the southeast, southern and southwest margins (Heap and Harris, 2008). In contrast, fewer canyons have formed in those areas of the Australian margin with a lower gradient slope, such as along the prograded carbonate platform in the Great Australian Bight where slope failure appears less well developed (Feary and James, 1998; Hill et al., 2005). While many canyons on the Australian margin have formed by a common process and are ancient features, they will have formed at varying rates depending on underlying geological controls. This variability is reflected in the wide range in size and complexity of slope-confined canyons in particular, a pattern represented in the classification results from this study. In particular, the classes of the data-driven EM classification derived from shape and location metrics (Fig. 11) together describe canyons that range from small, narrow and shallow canyons at the early stage of evolution to large, complex and deep canyons with multiple tributaries that are clearly more advanced in

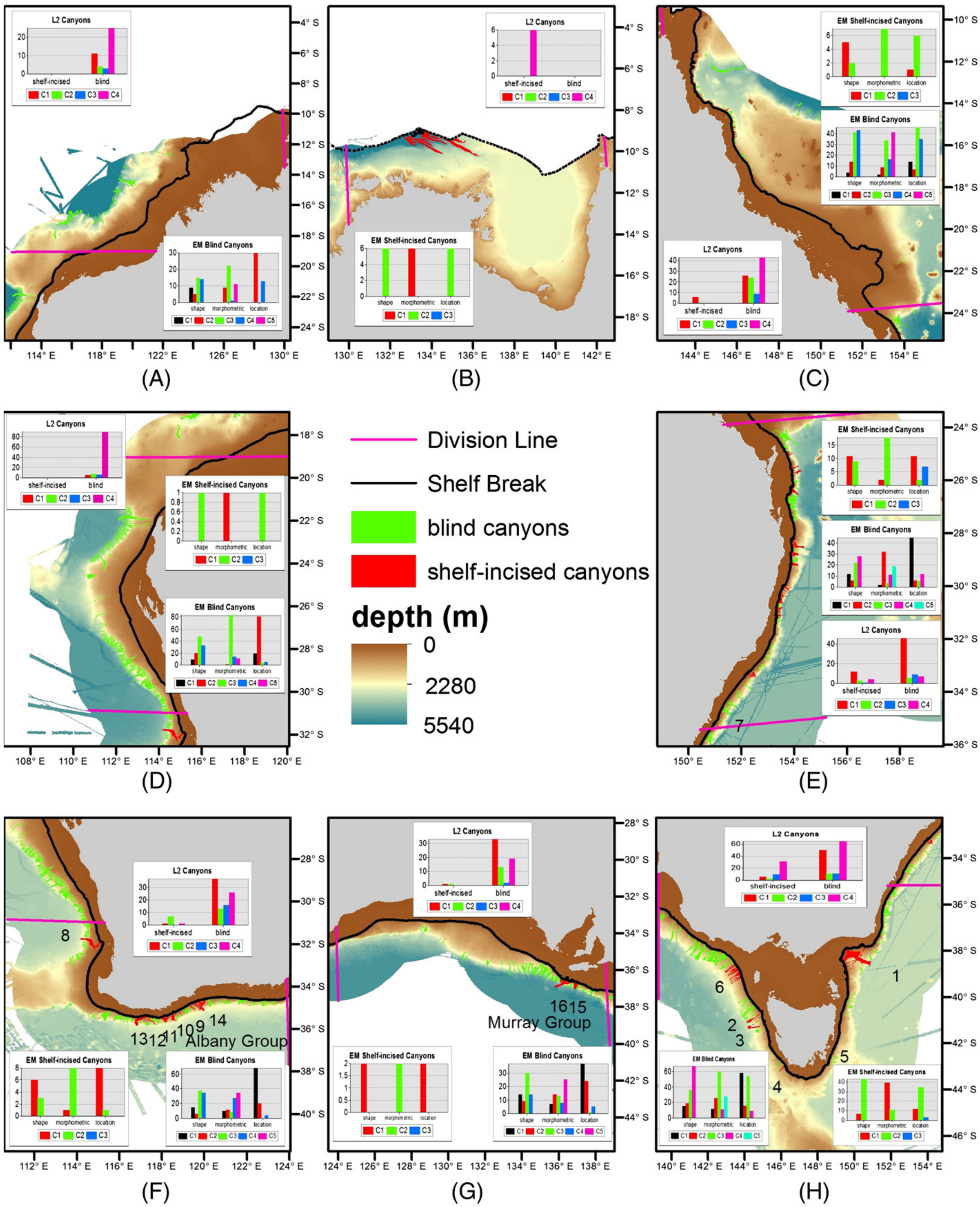

L2 Canyons
EM Blind Canyons
EM Shelf-incised Canyons
shelf-incised
blind
shape
morphometric
location
C1
C2
C3
C4
C5
Division Line
Shelf Break
blind canyons
shelf-incised canyons
depth (m)
0
2280
5540
Albany Group
Murray Group
(A)
(B)
(C)
(D)
(E)
(F)
(G)
(H)

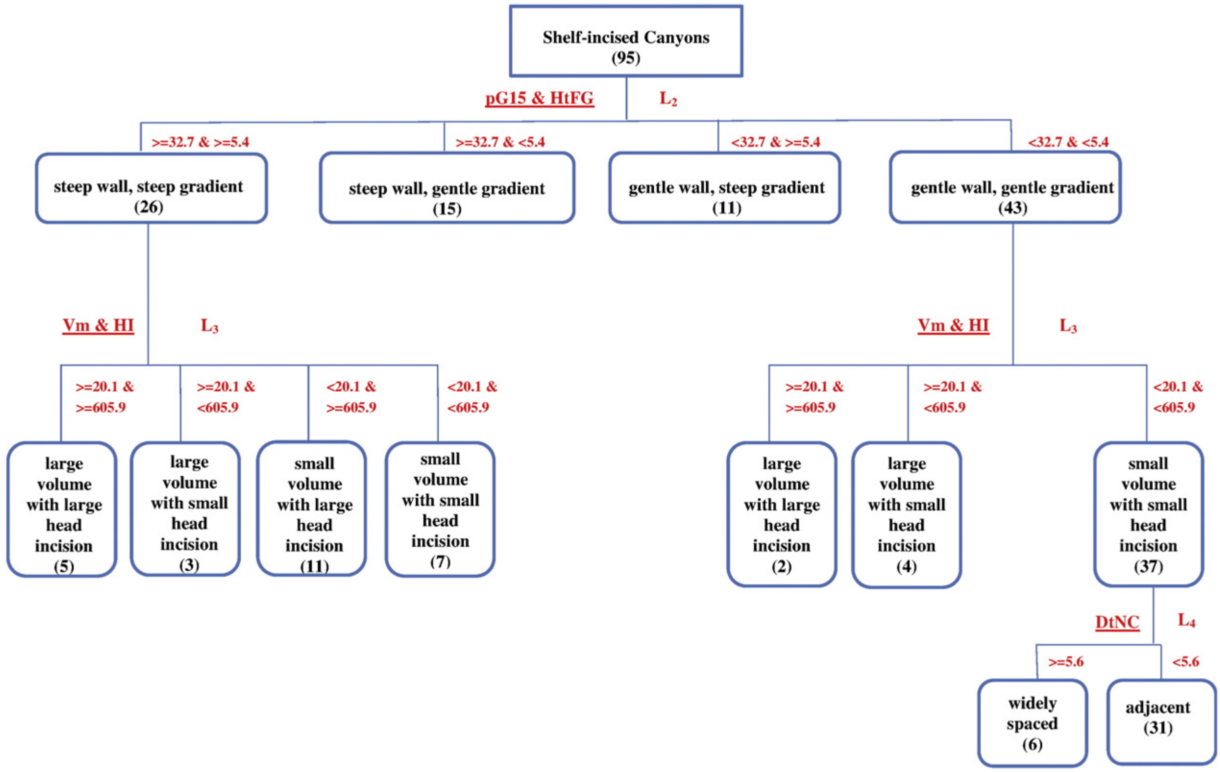

Fig. 6. Hierarchical classification tree for shelf-incising canyons based on knowledge-driven classification. Numbers in brackets indicate the number of canyons in each class. The classification levels and the boundary values of the selected canyon metrics are also shown.

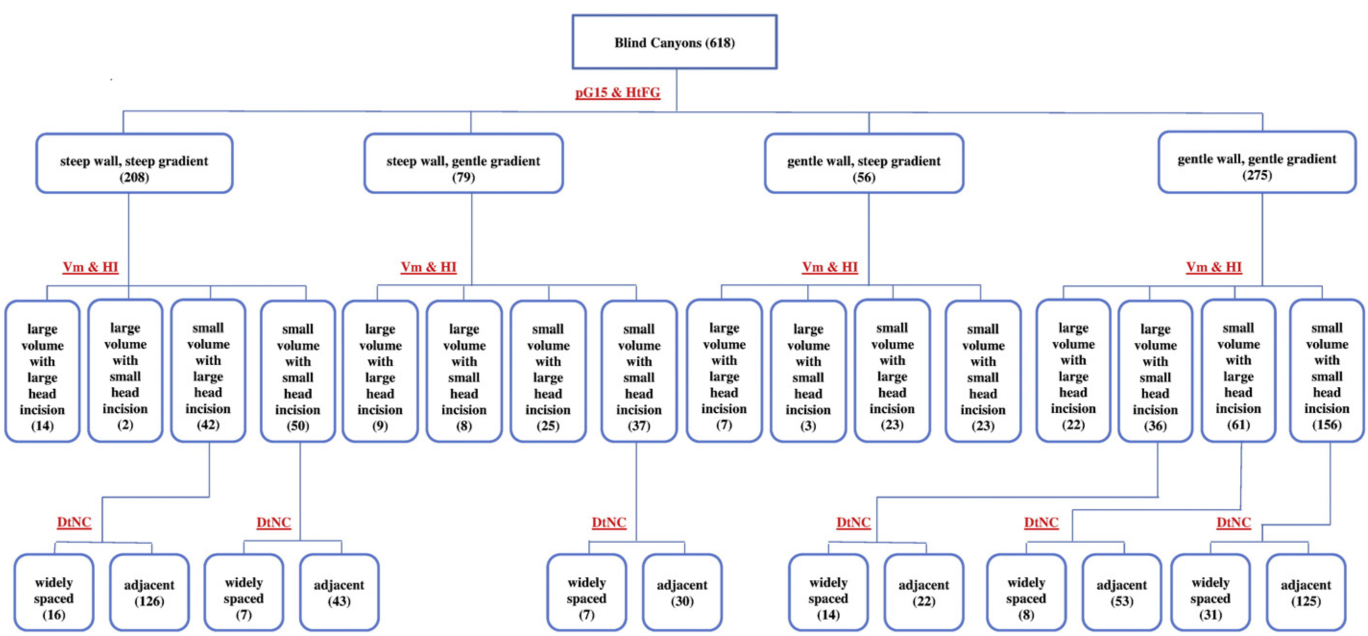

Fig. 7. Hierarchical classification tree for blind canyons based on knowledge-driven classification. Numbers in brackets indicate the number of canyons in each class.

Fig. 5 Spatial distribution of shelf-incising and blind canyons within the eight geographic regions; (a) northwest; (b) north; (c) northeast; (d) west; (e) east; (f) southwest; (g) south; (h) southeast. The vertical-bar diagrams in each panel show the canyon numbers of different classes for the geographic region; The bar diagram titled "L2 Canyons" compares the shelf-incising canyons and the blind canyons based on the L_2 classification results (knowledge-driven) (C1—"steep wall, steep gradient", C2—"steep wall, gentle gradient", C3—"gentle wall, steep gradient", C4—"gentle wall, gentle gradient"); The bar diagram titled "EM Shelf-incising Canyons" displays the EM clustering results of the shelf-incising canyons based on the Shape, Morphometric and Location metrics (C1—cluster 1, C2—cluster 2, C3—cluster 3); The bar diagram titled "EM Blind Canyons" displays the EM clustering results of the blind canyons based on the Shape, Morphometric and Location metrics (C1—cluster 1, C2—cluster 2, C3—cluster 3, C4—cluster 4, C5—cluster 5). Named shelf-incising canyons are numbered as follows: 1—the Bass Canyon system, 2—Ling Hole Canyon, 3—Pieman Canyon, 4—Southwest Canyon, 5—Riedle Canyon, 6—King Island Canyon, 7—Long Nose Canyon, 8—Perth Canyon, 9—Pallinup Canyon, 10—Mermaid Canyon, 11—Kalgan Canyon, 12—Denmark Canyon, 13—Wilson Canyon, 14—Bremer Canyon, 15—Sprigg Canyon and 16—Du Couedic Canyon.

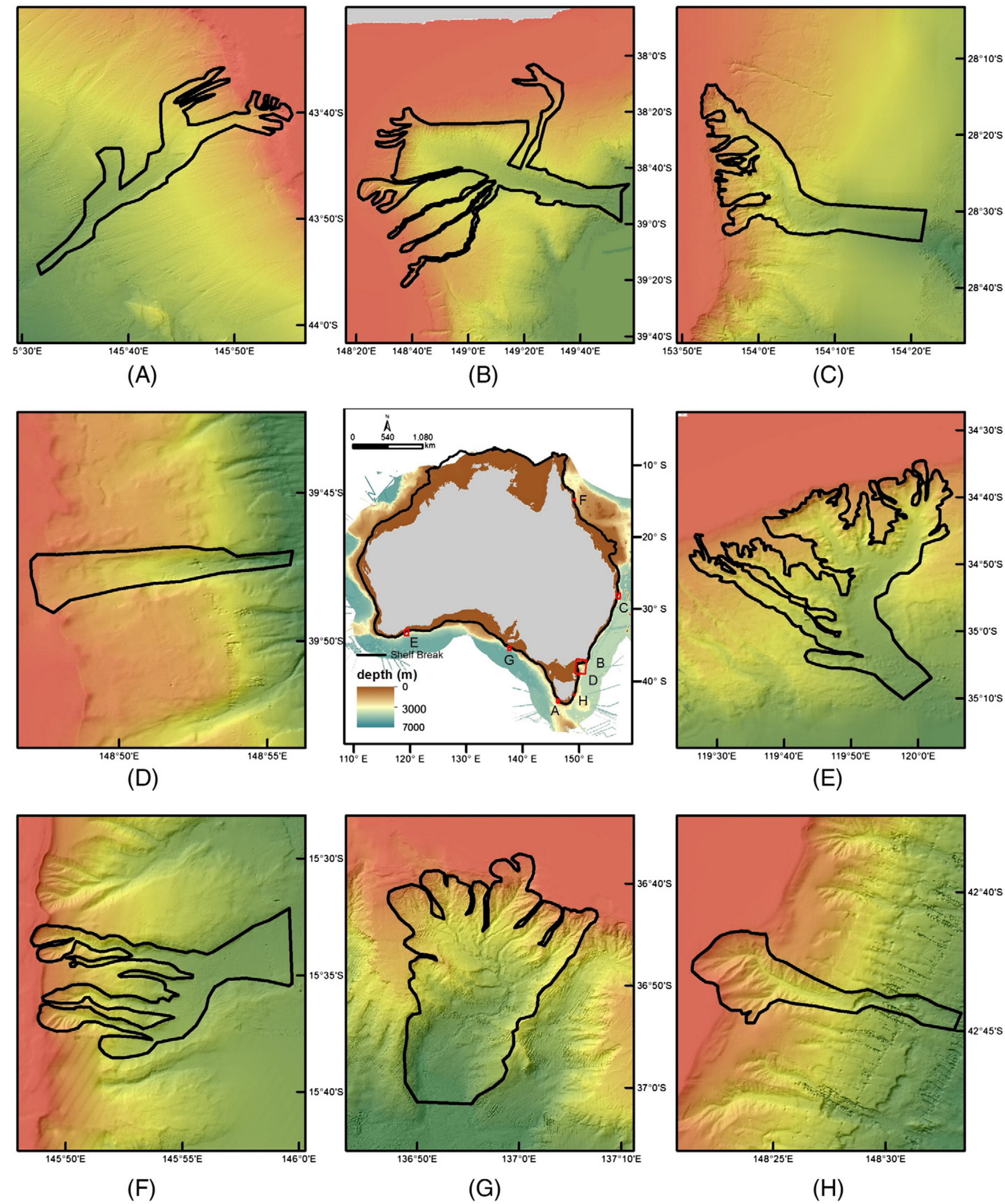

Fig. 8. The locations and images of the representative shelf-incising canyons in different knowledge-driven classes; (a) Southwest Cape Canyon ("gentle wall, gentle gradient" and "small volume with small head incision"); (b) Bass Canyon ("gentle wall, gentle gradient" and "large volume with small head incision"); (c) an unnamed canyon ("gentle wall, gentle gradient" and "large volume with large head incision"); (d) Coral Canyon ("gentle wall, steep gradient"); (e) Bremer Canyon ("steep wall, gentle gradient"); (f) an unnamed canyon ("steep wall, steep gradient" and "small volume with large head incision"); (g) Sprigg Canyon ("steep wall, steep gradient" and "large volume with small head incision"); (h) Riedle Canyon ("steep wall, steep gradient" and "small volume with small head incision").

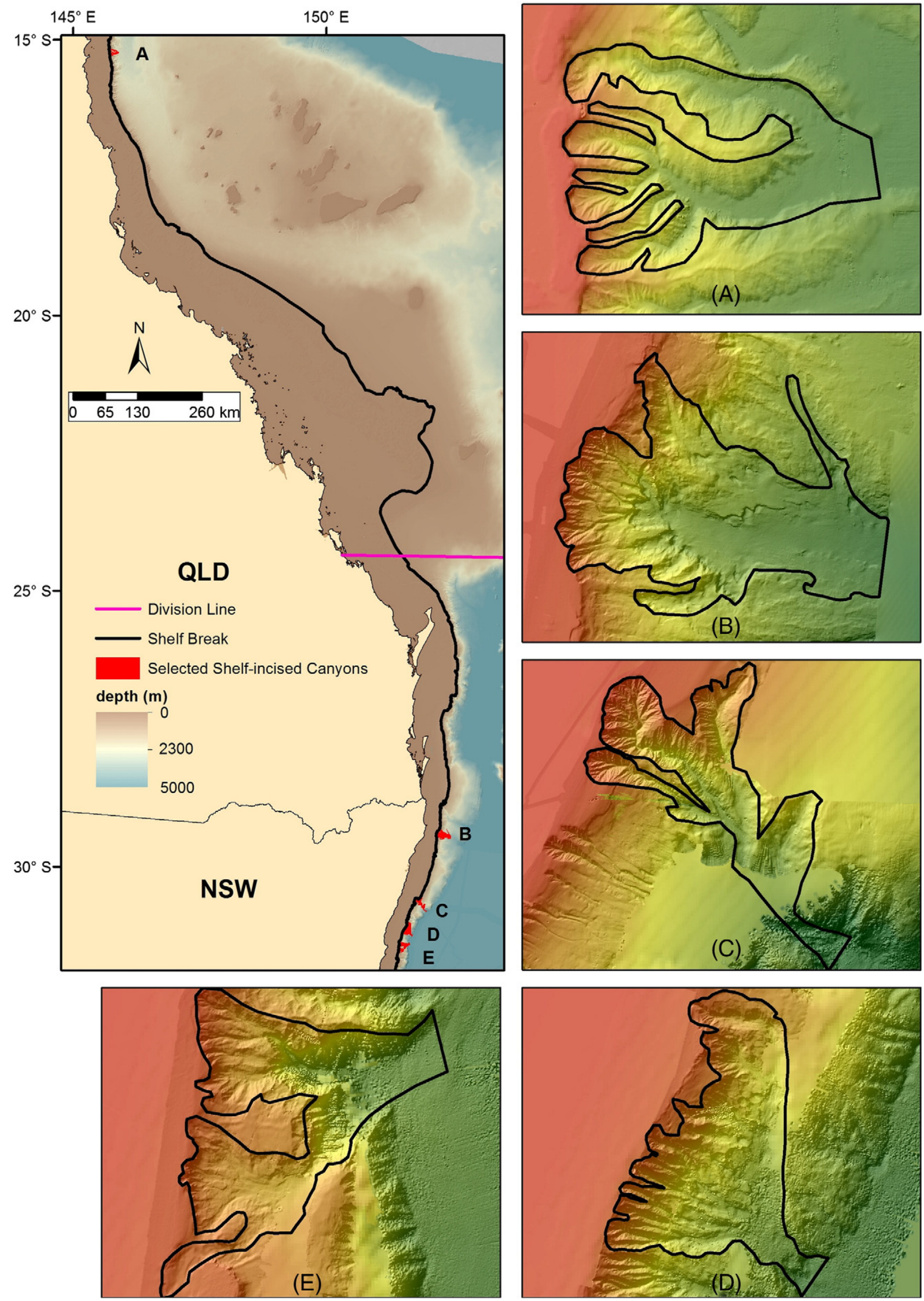

Fig. 9. The locations of the five most complex shelf-incising canyons in the class of "steep wall, steep gradient" and "large volume with large head incision" (Fig. 6) and their images.

Table 5
The statistics of canyon metrics for the five most complex shelf-incised canyons in the class of "steep wall, steep gradient" and "large volume with large head incision". The locations and images of these five canyons are shown in Fig. 9.

ID	1	2	3	4	5	Mean	STD
Pm	145.1	143.0	145.7	119.6	135.9	137.9	10.9
PA	153.7	377.8	234.0	304.2	275.2	269.0	83.1
CL	79.3	120.6	85.8	95.1	116.8	99.5	18.5
MbrW	14.2	23.5	18.7	21.8	22.9	20.2	3.8
MbrL	19.3	30.1	34.2	27.3	28.2	27.8	5.5
MbrO	81.6	99.2	128.9	13.9	6.9	66.1	53.6
LtWR	1.4	1.3	1.8	1.3	1.2	1.4	0.2
BI	2.2	1.3	1.4	1.2	1.3	1.5	0.4
Cp	1.8	1.9	2.7	2.0	2.3	2.1	0.4
NoB	9.0	9.0	8.0	10.0	9.0	9.0	0.7
HI	873.0	780.0	684.0	658.0	674.0	733.8	91.3
HD	−44.0	−187.0	−144.0	−465.0	−288.0	−225.6	159.9
FD	−2271.0	−3293.0	−4443.0	−4395.0	−4267.0	−3733.8	943.2
DR	2227.0	3106.0	4299.0	3930.0	3979.0	3508.2	840.9
AG	17.0	12.8	19.4	19.7	19.6	17.7	3.0
StdG	10.4	10.0	10.4	11.0	13.6	11.1	1.5
RG	68.9	67.0	83.8	81.4	79.7	76.2	7.7
SA	171.0	401.0	291.6	371.1	356.3	318.2	91.5
Rg	1.1	1.1	1.2	1.2	1.3	1.2	0.1
Vm	21.0	97.4	52.6	89.9	95.8	71.3	33.6
HtFD	19,507.9	30,053.0	31,467.3	29,489.4	21,858.8	26,475.3	5400.5
HtFG	6.5	5.9	7.8	7.6	10.3	7.6	1.7
DtNC	0.3	0.8	4.2	0.2	0.4	1.2	1.7
FV	19.0	9.0	13.0	14.0	15.0	14.0	3.6
ID	−548.8	−597.5	−487.9	−767.4	−750.4	−630.4	123.7
IA	20.1	34.2	34.2	24.0	49.9	32.5	11.5
pG15	58.4	35.2	64.5	61.8	53.7	54.7	11.6
Sn	4.1	4.0	2.7	3.2	5.3	3.9	1.0
DtRM	96.2	37.5	30.3	31.9	41.8	47.5	27.6

their development. As such, these classes provide an objective, quantitative framework for future studies aimed at better understanding the geological controls on canyon evolution at local to regional scales, including finer scale analysis of canyon geomorphology from multibeam bathymetry data as undertaken by Brothers et al. (2013) for the US margin.

7.3. Canyons, currents and biodiversity

In the canyon classification procedure used here, shelf-incising canyons were treated separately from blind canyons on the basis that the former provide more diverse marine habitats and intersect major ocean boundary currents on the Australian margin. The shelf-incising canyons mapped here are generally larger in size and depth-range than the blind canyons (Table 2), and are more likely to have mixed hard and soft substrates. As a result, some shelf-incising canyons in Australia have been shown to harbour high biodiversity (e.g., Schlacher et al., 2007; S. Rennie et al., 2009; Currie and Sorokin, 2014). For example, Schlacher et al. (2007) found that King Island Canyon, Ling Hole Canyon, Pieman Canyon and a branch of Bass Canyon on the south-eastern margin (Fig. 5h) support a rich sponge fauna. They attributed this high sponge diversity to the heterogeneous habitats provided by these canyons. Another study showed that Du Couedic Canyon, which is a shelf-incising canyon on the southern margin (Fig. 5g), has much higher megafaunal diversity than the slope-confined Bonney Canyon in the same region (Currie and Sorokin, 2014). This is likely because Du Couedic Canyon is much larger in size (planar area 1689 km^2, depth range 4922 m), more complex in morphology (25 branches) and closer to adjacent canyons (0.2 km) than Bonney Canyon (area 204 km^2, single branch, depth range 728 m and 10.6 km to nearest canyon).

Many of the shelf-incising canyons also intersect the Leeuwin Current (and Leeuwin Undercurrent), Flinders Current and East Australian Current. Associated hydrodynamics such as upwelling enhance the horizontal and vertical exchanges of water and materials between the slope and shelf (Allen et al., 2001; Jordi et al., 2005; Kampf, 2007). The proximity of some shelf-incising canyons to the coast could also facilitate the transportation of nutrient-rich coastal sediment to the deep sea through gravity flows and cascading events documented in Australia and elsewhere (e.g., Canals et al., 2006; Zuniga et al., 2009; Middleton and Bye, 2007; Pattiaratchi et al., 2011). We discuss several examples below.

Perth Canyon on the south-western margin (Figs. 2; 5f) is the second largest canyon on the Australian margin and one of the most studied. In this study, it is one of a group of eight canyons in the southwest region that are classified as topographically complex (i.e. EM cluster 2 — large head incision, steep and rugose; Fig. 5f). Recent modelling and observation studies show that the Perth Canyon interacts strongly with the Leeuwin Undercurrent which leads to eddy generation at 400–800 m depth and upwelling (S.J. Rennie et al., 2009; S. Rennie et al., 2009). As a result, a high productivity layer (at depth of ~200 m) is formed just under the Leeuwin Current which is downwelling favourable. During summer, the Leeuwin Current is typically weaker and strong northerly winds act to promote vertical mixing that brings nutrients to the surface layer (Feng et al., 2003). In addition, the circulation in the canyon is likely to be responsible for the aggregations of krill near the canyon head, providing a key food source for pygmy blue whales (S. Rennie et al., 2009). The role of upwelling in other topographically complex canyons that intersect the Leeuwin Undercurrent remains to be fully explored.

On the southern margin (Fig. 5g), the Flinders Current flows westward along the upper continental slope and promotes upwelling, particularly within the topographically complex canyons in the Murray group such as Du Couedic Canyon described above (Middleton and Cirano, 2002; Kampf, 2006; Middleton and Bye, 2007; Kampf, 2010; Currie et al., 2012). This deep canyon upwelling from depths of ~250 m helps to form a large sub-surface nutrient pool known as the Kangaroo Island pool (Middleton and Bye, 2007; Kampf, 2010). During summer, coastal wind-forced upwelling brings this nutrient-rich water closer to the coast to form the Bonney Coast upwelling and Eyre Peninsula upwelling regions which are recognised as Key Ecological Features (Commonwealth of Australia, 2013b). Again, the extent to which this process is active in other canyons with similar morphometric characteristics in this region requires further investigation.

The East Australian Current flows southward along the shelf break with significant hydrological and biological effects (Brassington et al., 2011; Suthers et al., 2011). It intensifies between 22°S and the separation zone (31°S–32°S) then declines to about 45°S (Ridgway and Dunn, 2003). Although the influence of regional topography on the East Australian Current has been demonstrated in Ridgway and Dunn (2003), the interaction between the East Australian Current and individual canyons has yet to be studied. It is likely though, that the canyons on the eastern and south-eastern margins (Fig. 5e, h) would also generate canyon upwelling with the similar mechanisms of the southern margin (Condie, 1995; Roughan and Middleton, 2004; Baird et al., 2006; Kampf, 2010). In particular, the East Australian Current experiences significant variability with eddy activities around the separation zone (Bowen et al., 2005; O'Kane et al., 2011) where several shelf-incising canyons (including 3 of the 5 most complex canyons) are located (Figs. 5e; 9). This variability of the East Australian Current through eddy activity likely promotes vertical mixing and enhances nutrient flux to this area which is known to have significant coastal upwelling (Oke and Middleton, 2001).

The new submarine canyon dataset also provides for an assessment of the extent to which these seabed features are represented in the national network of marine protected areas, established by Australia in 2012. Designed to protect marine biodiversity within the Australian marine jurisdiction, the network of Commonwealth Marine Reserves (CMR) covers 3.1 million km^2 with reserves on all sides of the continent (Fig. 3). We calculate that 36% (n = 254) of the canyons in the new canyon dataset intersects a CMR. For the shelf-incising canyons, which are typically more biologically productive, a similar proportion (34%) intersects a CMR. In terms of the spatial distribution of CMR-canyons, the

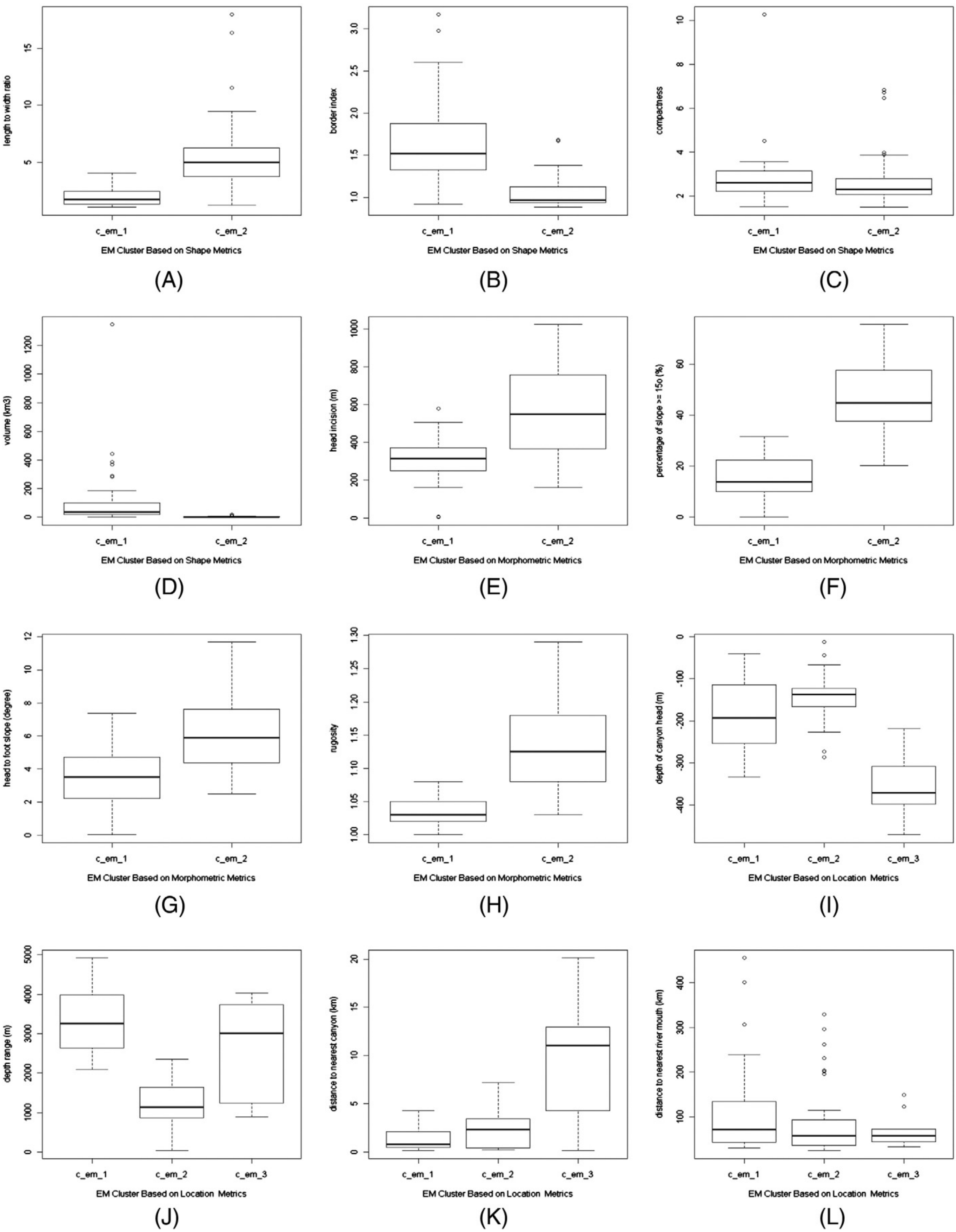

Fig. 10. Boxplots of metrics for EM-derived classes of shelf-incising canyons: (a) LtWR; (b) BI; (c) Cp; (d) Vm; (e) HI; (f) pG15; (g) HtFG; (h) Rg; (i) HD; (i) DR; (k) DtNC; (l) DtRM. The thick line in the middle of each box is the median value for each parameter, with the 25th and 75th percentiles represented at the top and bottom of each box, respectively. The range of data is represented by the whiskers (dotted lines) outside the boxes. Circles represent outliers that are more than 1.5 times the interquartile range.

Table 6
Significance tests of the selected canyon metrics for the separation of EM clusters.

		Shelf-incised canyons		Blind canyons	
		F value	Significance[1]	F value	Significance
Shape metrics	LtWR	42.7	Yes	62.2	Yes
	BI	66.5	Yes	103.9	Yes
	Cp	0.66	No	47.7	Yes
	Vm	17	Yes	116	Yes
Morphometrics	HI	45.8	Yes	256.2	Yes
	pG15	205.4	Yes	361.7	Yes
	HtFG	40.7	Yes	299.4	Yes
	Rg	102.3	Yes	235.9	Yes
Location metrics	HD	46.3	Yes	157.7	Yes
	DR	82.8	Yes	95.4	Yes
	DtNC	42.3	Yes	46.2	Yes
	DtRM	1.6	No		
	DtSB			181.9	Yes

[1] At 99% significant level.

continent-wide pattern is reflected in relative terms, with CMRs in the southeast and southwest marine regions each covering 8% (n = 54 and 60, respectively) of the mapped canyon population, whereas CMRs in the north marine region include 1% (n = 5). This information has potential application in supporting the setting of priorities for management and monitoring of the CMR network, such as the analysis of the relative importance of a canyon, or group of canyons, in providing conditions that promote primary productivity and in turn biodiversity.

7.4. Increasing the inventory and reducing uncertainty in canyon mapping

This study has increased the number of recognised submarine canyons on the Australian margin by approximately 75%, to 713 from the 405 mapped by Heap and Harris (2008). The majority of these additions to the dataset were either not identifiable in the previous 250 m bathymetry grid (Heap and Harris, 2008), or have now been mapped as individual canyons, as they were not resolvable as such previously. We are confident that the criteria used in this study have not introduced features that were mapped as valleys by Heap and Harris (2008) because all the valleys in that dataset fall outside the canyon criteria. The increased canyon count is therefore attributed here to better resolution bathymetry data. Importantly, the pattern in the spatial distribution of submarine canyons on the Australian margin, as described by Heap and Harris (2008), is maintained by this new canyon dataset.

The quality of the bathymetry datasets used here for canyon mapping clearly determines the uncertainty of the results presented. The national bathymetry grid (Whiteway, 2009) and the bathymetry grid of the Great Barrier Reef and Coral Sea regions (Beaman, 2010) used variable data sources. Among these data sources, the modelled data and satellite derived data are less reliable in depth estimation. In the present study, multibeam surveys cover large sections of the outer continental shelf to upper continental slope, where most submarine canyons are located (Figs. 1 and 3). This resulted in 78% of mapped submarine canyons with low and acceptable uncertainty levels (scores 1, 2 and 3; Table 4). More importantly, 94% of the shelf-incising canyons has been mapped with low and acceptable uncertainty. With this information it is possible to establish priorities for future multibeam surveys of submarine canyons. For example, priority could be given to mapping the 10 shelf-incising canyons with an uncertainty score of 3 and to the large number of blind canyons that have uncertainty scores of 3 or 4 (248 and 106, respectively). This would lift the mapping quality of an additional 50% of Australia's submarine canyons to a satisfactory level. It would also provide the basis for more comprehensive interpretations of the fine-scale geomorphology within canyons that is necessary to better understand canyon evolution.

8. Conclusions and future work

The results of this study confirm the physical diversity of Australian submarine canyons, with the major findings as follows:

- New and updated bathymetric data allowed mapping of 713 canyons on the Australian margin, with 95 of these identified as shelf-incising and the remainder confined to the continental slope;
- The spatial distribution of submarine canyons is irregular, with more canyons located on the steeper and narrow shelf and slope of the eastern, western and southern margins of Australia;
- Shelf-incising canyons have different geometric (shape), morphometric and location characteristics from blind canyons beyond their positioning on the continental margin;
- Canyon metrics describe a wide variety of canyon form and complexity that is consistent with a population of canyons that has evolved at different rates around the Australian margin since the break-up of Gondwana.
- The large number of slope-confined canyons is interpreted to reflect dominance of slope mass-wasting processes over erosive turbidity flows from fluvial and shelf sources on an arid continent.
- Submarine canyons are well represented in the Commonwealth of Australia's national network of marine protected areas, with 36% of the mapped canyons intersecting a Commonwealth Marine Reserve;

These results underpin future investigations of ecological processes and functions of Australian submarine canyons. In particular, the establishment of a hierarchy of canyon types provides an objective framework for observation and hypothesis-testing, and for placing local case studies into a broader context.

Acknowledgements

This work was undertaken for the Marine Biodiversity Hub, a collaborative partnership supported through funding from the Australian Government's National Environmental Research Program (NERP). NERP Marine Biodiversity Hub partners include the Institute for Marine and Antarctic Studies, University of Tasmania; CSIRO, Geoscience Australia, Australian Institute of Marine Science, Museum Victoria, Charles Darwin University and the University of Western Australia. We would like to thank the following people for their help in forming the ideas and techniques of this study: Nix Bax, Jessica Meeuwig, Johnathan Kool, Tom Letessier, Phil Bouchet, Rudy Kloser and Gordon Keith. Valuable reviews by Jin Li and Tony Nicholas of Geoscience Australia, Danny Brothers and an anonymous reviewer have improved the manuscript. This paper is published with permission of the Chief Executive Officer, Geoscience Australia.

References

Akaike, H., 1974. A new look at the statistical model identification. IEEE Transactions on Automatic Control 19, 716–723.

Ali, J.R., Aitchison, J.C., 2005. Greater India. Earth-Science Reviews 72, 169–188.

Allen, S.E., Vindeirinho, C., Thomson, R.E., Foreman, M.G.G., Mackas, D.L., 2001. Physical and biological processes over a submarine canyon during an upwelling event. Canadian Journal of Fisheries and Aquatic Sciences 58, 671–684.

Baird, M.E., Timko, P.G., Suthers, I.M., Middleton, J.H., 2006. Coupled physical–biological modelling study of the East Australian Current with idealised wind forcing. Part I: biological model intercomparison. Journal of Marine Systems 59, 249–270.

Beaman, R.J., 2010. Project 3DGBR: a high-resolution depth model for the Great Barrier Reef and Coral Sea. Marine and Tropical Sciences Research Facility (MTSRF) Project 2.5i.1a Final ReportMTSRF, Cairns, Australia, p. 13 (plus Appendix 1).

Bosley, K.L., Lavelle, J.W., Brodeur, R.D., Wakefield, W.W., Emmett, R.L., Baker, E.T., Rehmke, K.M., 2004. Biological and physical processes in and around Astoria submarine Canyon, Oregon, USA. Journal of Marine Systems 50, 21–37.

Bourget, J., Zaragosi, S., Garlan, T., Gabelotaud, I., Guyomard, P., Dennielou, B., Ellouz-Zimmermann, N., Schneider, J.L., 2008. Discovery of a giant deep-sea valley in the Indian Ocean, off eastern Africa: the Tanzania channel. Marine Geology 255, 179–185.

Bowen, M.M., Wilkin, J.L., Emery, W.J., 2005. Variability and forcing of the East Australian Current. Journal of Geophysical Research 110, C03019.

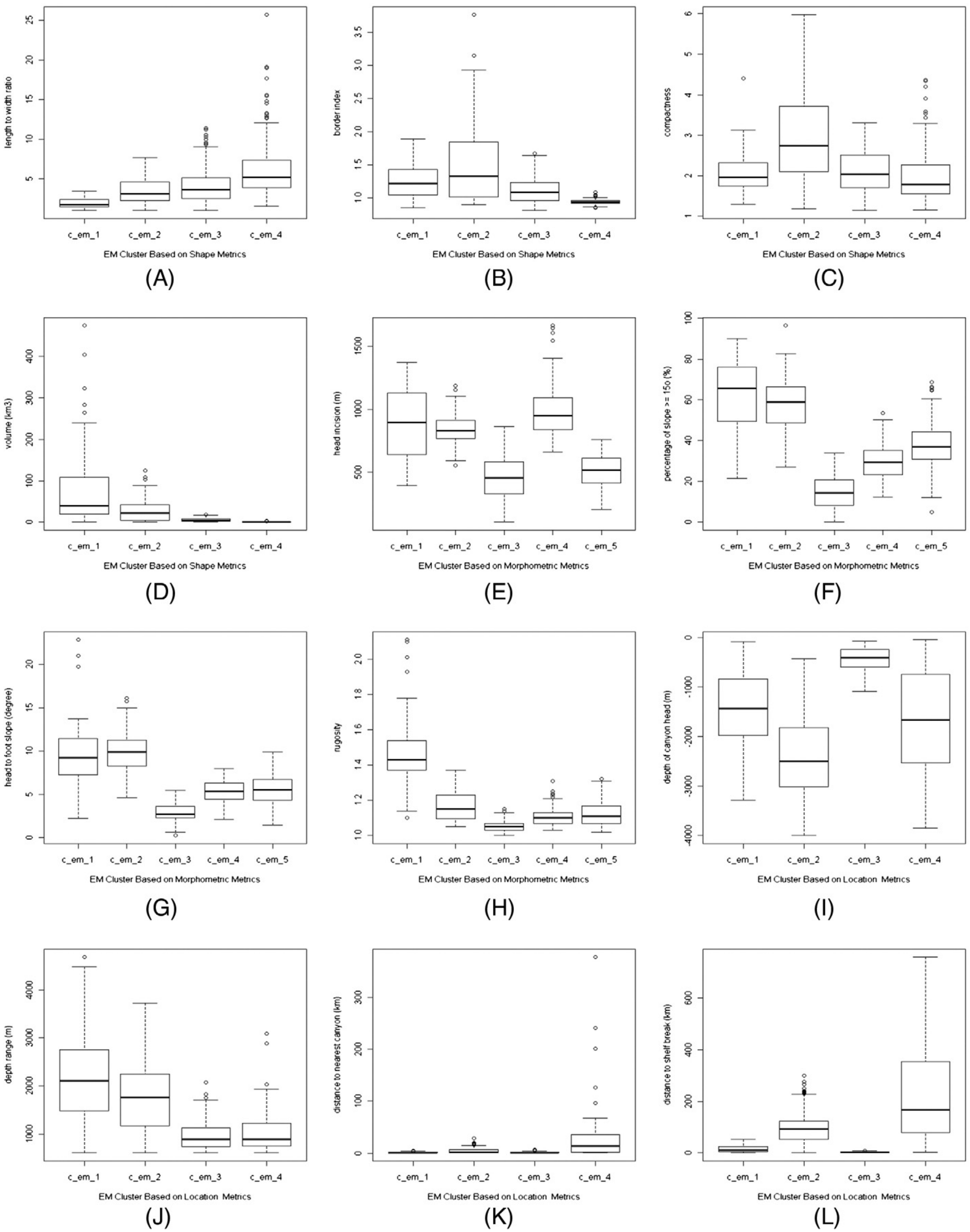

Fig. 11. Boxplots of metrics for EM-derived classes of blind canyons: (a) LtWR; (b) BI; (c) Cp; (d) Vm; (e) HI; (f) pG15; (g) HtFG; (h) Rg; (i) HD; (i) DR; (k) DtNC; (l) DtSB. The thick line in the middle of each box is the median value for each parameter, with the 25th and 75th percentiles represented at the top and bottom of each box, respectively. The range of data is represented by the whiskers (dotted lines) outside the boxes. Circles represent outliers that are more than 1.5 times the interquartile range.

Brassington, G.B., Summons, N., Lumpkin, R., 2011. Observed and simulated Lagrangian and eddy characteristics of the East Australian Current and the Tasman Sea. Deep-Sea Research II 58, 559–573.
Brodeur, R.D., 2001. Habitat-specific distribution of Pacific ocean perch (*Sebastes alutus*) in Pribilof Canyon, Bering Sea. Continental Shelf Research 21, 207–224.
Brothers, D.S., ten Brink, U.S., Andrews, B.D., Chaytor, J.D., Twichell, D.C., 2013. Geomorphic process fingerprints in submarine canyons. Marine Geology 337, 53–66.
Butler, A., Harris, P., Lyne, V., Heap, A., Passlow, V., Porter-Smith, R., 2001. An Interim Bioregionalisation for the continental slope and deeper waters of the South-East Marine Region of Australia. Report to the National Oceans Office, Commonwealth of Australia.
Cacchione, D.A., Pratson, L.F., Ogston, A.S., 2002. The shaping of continental slopes by internal tides. Science 296, 724–727.
Canals, M., Puig, P., de Madron, X.D., Heussner, S., Palanques, A., Fabres, J., 2006. Flushing submarine canyons. Nature 444, 354–357.
Carter, G.S., Gregg, M.C., 2002. Intense, variable mixing near the head of Monterey submarine canyon. Journal of Physical Oceanography 32, 3145–3165.
Cartes, J.E., Fanelli, E., Papiol, V., Maynou, F., 2010. Trophic relationships at intra-annual spatial and temporal scales of macro and megafauna around a submarine canyon off the Catalonian coast (western Mediterranean). Journal of Sea Research 63, 180–190.
Commonwealth of Australia, 2013a. Australia's network of Commonwealth marine reserves. http://www.environment.gov.au/marinereserves/pubs/map-national.pdf (accessed 12 June, 2013).
Commonwealth of Australia, 2013b. Key Ecological Features. http://www.environment.gov.au/metadataexplorer/full_metadata.jsp?docId=%7B093A2086-7DE3-41A7-B407-5BCCA7F400A5%7D&loggedIn=false (accessed 12 June, 2013).
Condie, S.A., 1995. Interactions between western boundary currents and shelf waters: a mechanism for coastal upwelling. Journal of Geophysical Research 100, 24811–24818.
Cunha, M.R., Paterson, G.L.J., Amaro, T., Blackbird, S., de Stigter, H.C., Ferreira, C., Glover, A., Hilario, A., Kiriakoulakis, K., Neal, L., Ravara, A., Rodrigues, C.F., Tiago, A., Billett, D.S.M., 2011. Biodiversity of macrofaunal assemblages from three Portuguese submarine canyons (NE Atlantic). Deep-Sea Research Part II: Topical Studies in Oceanography 58, 2433–2447.
Currie, D.R., Sorokin, S.J., 2014. Megabenthic biodiversity in two contrasting submarine canyons on Australia's southern continental margin. Marine Biology Research 10, 97–110.
Currie, D.R., McClatchie, S., Middleton, J.H., Nayar, S., 2012. Biophysical factors affecting the distribution of demersal fish around the head of a Submarine Canyon Off the Bonney Coast, South Australia. PLoS ONE 7, e30138.
Daniell, J., Jorgensen, D.C., Anderson, T., Borissova, I., Burq, S., Heap, A.D., Hughes, M., Mantle, D., Nelson, G., Nichol, S., Nicholson, C., Payne, D., Przeslawski, R., Radke, L., Siwabessy, J., Smith, C., 2010. Frontier basins of the West Australian continental margin: post-survey report of marine reconnaissance and geological sampling survey GA2476. Geoscience Australia Record 2009/38, Canberra (229 pp.).
De Leo, F.C., Smith, C.R., Rowden, A.A., Bowden, D.A., Clark, M.R., 2010. Submarine canyons: hotspots of benthic biomass and productivity in the deep sea. Proceedings of the Royal Society B 277, 2783–2792. http://dx.doi.org/10.1098/rspb.2010.0462.
De Leo, F.C., Drazen, J.C., Vetter, E.W., Rowden, A.A., Smith, C.R., 2012. The effects of submarine canyons and the oxygen minimum zone on deep-sea fish assemblages off Hawaii. Deep Sea Research, Part I: Oceanographic Research Papers 64, 54–70.
De Leo, F.C., Vetter, E.W., Smith, C.R., Rowden, A.A., McGranaghan, M., 2014. Spatial scale-dependent habitat heterogeneity influences submarine canyon macrofaunal abundance ad diversity off the Main and Northwest Hawaiian Islands. Deep Sea Research Part II: Topical Studies in Oceanography 104, 267–290.
De Mol, L., Van Rooij, D., Pirlet, H., Greinert, J., Frank, N., Quemmerais, F., Henriet, J.-P., 2011. Cold-water coral habitats in the Penmarc'h and Guilvinec Canyons (Bay of Biscay): deep-water versus shallow-water settings. Marine Geology 282, 40–52.
de Stigter, H.C., Boer, W., de Jesus Mendes, P.A., Jesus, C.C., Thomsen, L., van den Bergh, G.D., van Weering, T.C.E., 2007. Recent sediment transport and deposition in the NazarÃ Canyon, Portuguese continental margin. Marine Geology 246, 144–164.
Dempster, A., Laird, N., Rubin, D., 1977. Maximum likelihood from incomplete data via the EM algorithm. Journal of Royal Statistical Society Series B 39, 1–38.
Exon, N.F., Hill, P.J., Mitchell, C., Post, A., 2005. Nature and origin of the submarine Albany canyons off southwest Australia. Australian Journal of Earth Sciences 52, 101–115.
Farre, J.A., McGregor, B.A., Ryan, W.B.F., Robb, J.M., 1983. Breaching the shelfbreak passage from youthful to mature phase in submarine canyon evolution. SEPM Special Publication 33, 25–39.
Feary, D.A., James, N.P., 1998. Seismic stratigraphy and geological evolution of the Cenozoic, cool-water Eucla Platform, Great Australian Bight. American Association of Petroleum Geologists Bulletin 82, 792–816.
Feng, M., Meyers, G., Pearce, A., Wijffels, S., 2003. Annual and interannual variations of the Leeuwin Current at 32_S. Journal of Geophysical Research 108, 3355.
Freeman, H., Shapira, R., 1975. Determining the minimum-area encasing rectangle for an arbitrary closed curve. Communications of the ACM 18, 409–413.
Garcia, R., van Oevelen, D., Soetaert, K., Thomsen, L., De Stigter, H.C., Epping, E., 2008. Deposition rates, mixing intensity and organic content in two contrasting submarine canyons. Progress In Oceanography 76, 192–215.
Gardner, W.D., 1989a. Baltimore Canyon as a modern conduit of sediment to the deep sea. Deep-Sea Research 36, 323–358.
Gardner, W.D., 1989b. Periodic resuspension in Baltimore Canyon by focusing of internal waves. Journal of Geophysical Research 94, 18185–18194.
Genin, A., 2004. Bio-physical coupling in the formation of zooplankton and fish aggregations over abrupt topographies. Journal of Marine Systems 50, 3–20.
Gili, J.M., Pages, F., Bouillon, J., Palanques, A., Puig, P., Heussner, S., Calafat, A., Canals, M., Monaco, A., 2000. A multidisciplinary approach to the understanding of hydromedusan populations inhabiting Mediterranean submarine canyons. Deep-Sea Research I 47, 1513–1533.
Gingele, F.X., De Deckker, P., Hillenbrand, C.-D., 2004. Late Quaternary terrigenous sediments from the Murray Canyons area, South Australia and their implications for sea level change, palaeoclimate and palaeodrainage of the Murray–Darling Basin. Marine Geology 212, 183–197.
Godfrey, J.S., Jones, I.S.F., Maxwell, J.G.H., Scott, B.D., 1980. On the winter cascade from Bass Strait into the Tasman Sea. Australian Journal of Marine and Freshwater Research 31, 275–286.
Greene, C.H., Wiebe, P.H., Burczynski, J., Youngbluth, M.J., 1988. Acoustical detection of high-density krill demersal layers in the submarine canyons off Georges Bank. Science 241, 359–361.
Greene, H.G., Clake Jr., S.H., Kennedy, M.P., 1991. Tectonic evolution of submarine canyons along the California continental margin. In: Osborne, R.H. (Ed.), From *Shoreline* to Abyss: Contributions in Marine Geology in Honor of Francis Parker ShepardSEPM Special Publication. 46. Society for Sedimentary Geology, Tulsa, Oklahoma, pp. 231–248.
Guerra, A., Gonzalez, A.F., Pascual, S., Dawe, E.G., 2011. The giant squid *Architeuthis*: an emblematic invertebrate that can represent concern for the conservation of marine biodiversity. Biological Conservation 144, 1989–1997.
Hargrave, B.T., Kostylev, V.E., Hawkins, C.W., 2004. Benthic epifauna assemblages, biomass and respiration in The Gully region on the Scotian Shelf, NW Atlantic Ocean. Marine Ecology Progress Series 270, 55–70.
Harris, P.T., 2011. Biogeography, benthic ecology and habitat classification schemes. In: Harris, P.T., Baker, E.K. (Eds.), Seafloor Geomorphology as Benthic Habitat: GeoHab Atlas of Seafloor Geomorphic Features and Benthic Habitats. Elsevier, London, pp. 61–91.
Harris, P.T., Whiteway, T., 2009. High seas marine protected areas: Benthic environmental conservation priorities from a GIS analysis of global ocean biophysical data. Ocean & Coastal Management 52, 22–38.
Harris, P.T., Whiteway, T., 2011. Global distribution of large submarine canyons: geomorphic differences between active and passive continental margins. Marine Geology 285, 69–86.
Harris, P.T., Heap, A.D., Whiteway, T., Post, A., 2008. Application of biophysical information to support Australia's representative marine protected area program. Ocean & Coastal Management 51, 701–711.
Harris, P.T., McMillan-Lawler, M., Rupp, J., Baker, E.K., 2014. Geomorphology of the oceans. Marine Geology 352, 4–24.
Heap, A.D., Harris, P.T., 2008. Geomorphology of the Australian margin and adjacent seafloor. Australian Journal of Earth Science 55, 555–585.
Hill, P.J., Exon, N.F., Keene, J.B., Smith, S.M., 1998. The continental margin off east Tasmania and Gippsland: structure and development using new multibeam sonar data. Exploration Geophysics 29, 410–419.
Hill, P.J., De Deckker, P., Exon, N.F., 2005. Geomorphology and evolution of the gigantic Murray canyons on the Australian southern margin. Australian Journal of Earth Sciences 52, 117–136.
Hooker, S.K., Whitehead, H., Gowans, S., 1999. Marine protected area design and the spatial and temporal distribution of cetaceans in a submarine canyon. Conservation Biology 13, 592–602.
Hotchkiss, F.S., Wunsch, C., 1982. Internal waves in Hudson Canyon with possible geological implications. Deep-Sea Research (Part A) 29, 415–442.
Huang, Z., Brooke, B.P., Harris, P.T., 2011. A new approach to mapping marine benthic habitats using physical environmental data. Continental Shelf Research 31, S4–S16.
Huvenne, V.A.I., Davies, J.S., 2013. Towards a new integrated approach to submarine canyon research. Deep-Sea Research Part II: Topical Studies in Oceanography http://dx.doi.org/10.1016/j.dsr2.2013.09.012.
Jenness, J.S., 2004. Calculating landscape surface area from digital elevation models. Wildlife Society Bulletin 32, 829–839.
Jordi, A., Orfila, A., Basterretxea, G., Tintore, J., 2005. Shelf-slope exchanges by frontal variability in a steep submarine canyon. Progress In Oceanography 66, 120–141.
kampf, J., 2006. Transient wind-driven upwelling in a submarine canyon: a process-oriented modelling study. Journal of Geophysical Research 111, C11011.
Kampf, J., 2007. On the magnitude of upwelling fluxes in shelf-break canyons. Continental Shelf Research 27, 2211–2223.
Kampf, J., 2010. On preconditioning of coastal upwelling in the eastern Great Australian Bight. Journal of Geophysical Research 115, C12071.
Kiriakoulakis, K., Blackbird, S., Ingels, J., Vanreusel, A., Wolff, G.A., 2011. Organic geochemistry of submarine canyons: the Portuguese Margin. Deep-Sea Research Part II: Topical Studies in Oceanography 58, 2477–2488.
Klinck, J.M., 1996. Circulation near submarine canyons: a modelling study. Journal of Geophysical Research 101, 1211–1223.
Kunze, E., Rosenfeld, L.K., Carter, G.S., Gregg, M.C., 2002. Internal waves in Monterey submarine canyon. Journal of Physical Oceanography 32, 1890–1913.
Louzao, M., Anadon, N., Arrontes, J., Alvarez-Claudio, C., Fuente, D.M., Ocharan, F., Anadon, A., Acuna, J.L., 2010. Historical macrobenthic community assemblages in the Aviles Canyon, N Iberian Shelf: baseline biodiversity information for a marine protected area. Journal of Marine Systems 80, 47–56.
Ludwig, W., Probst, J.-L., 1998. River sediment discharge to the oceans: present-day controls and global budgets. American Journal of Science 298, 265–295.
Martin, J., Palanques, A., Vitorino, J., Oliveira, A., de Stigter, H.C., 2011. Near-bottom particulate matter dynamics in the Nazare submarine canyon under calm and stormy conditions. Deep-Sea Research Part II: Topical Studies in Oceanography 58, 2388–2400.
McClain, C.R., Barry, J.P., 2010. Habitat heterogeneity, disturbance, and productivity work in concert to regulate biodiversity in deep submarine canyons. Ecology 91, 964–976.
Mendes, C.R., Sa, C., Vitorino, J., Borges, C., Tavano Garcia, V.M., Brotas, V., 2011. Spatial distribution of phytoplankton assemblages in the Nazare submarine canyon region (Portugal): HPLC-CHEMTAX approach. Journal of Marine Systems 87, 90–101.

Middleton, J.F., Bye, J.A.T., 2007. A review of the shelf-slope circulation along Australia's southern shelves: Cape Leeuwin to Portland. Progress In Oceanography 75, 1–41.
Middleton, J.F., Cirano, M., 2002. A northern boundary current along Australia's southern shelves: the Flinders Current. Journal of Geophysical Research 107, 3129.
Mitchell, J.K., Holdgate, G.R., Wallace, M.W., 2007. Pliocene–Pleistocene history of the Gippsland Basin outer shelf and canyon heads, southeast Australia. Australian Journal of Earth Sciences 54, 49–64.
O'Kane, T.J., Oke, P.R., Sandery, P.A., 2011. Predicting the East Australian Current. Ocean Modelling 38, 251–266.
Oke, P.R., Middleton, J.H., 2001. Nutrient enrichment off Port Stephens: the role of the East Australian Current. Continental Shelf Research 21, 587–606.
Palanques, A., Garcia-Ladona, E., Gomis, D., Martin, J., Marcos, M., Pascual, A., Puig, P., Gili, J.-M., Emelianov, M., Monserrat, S., Guillen, J., Tintore, J., Segura, M., Jordi, A., Ruiz, S., Basterretxea, G., Font, J., Blasco, D., Pages, F., 2005. General patterns of circulation, sediment fluxes and ecology of the Palames (La Fonera) submarine canyon, northwestern Mediterranean. Progress In Oceanography 66, 89–119.
Paterson, G.L.J., Glover, A.G., Cunha, M.R., Neal, L., de Stigter, H.C., Kiriakoulakis, K., Billett, D. S.M., Wolff, G.A., Tiago, A., Ravara, A., Lamont, P., Tyler, P., 2011. Disturbance, productivity and diversity in deep-sea canyons: a worm's eye view. Deep-Sea Research Part II: Topical Studies in Oceanography 58, 2448–2460.
Pattiaratchi, C., Hollings, B., Woo, M., Welhena, T., 2011. Dense shelf water formation along the south-west Australian inner shelf. Geophysical Research Letters 38, L10609.
Porter-Smith, R., Lyne, V.D., Kloser, R.J., Lucieer, V.L., 2012. Catchment-based classification of Australia's continental slope canyons. Marine Geology 303–306, 183–192.
Puga-Bernabeu, A., Webster, J.M., Beaman, R.J., Guilbaud, V., 2011. Morphology and controls on the evolution of a mixed carbonate-siliciclastic submarine canyon system, Great Barrier Reef margin, north-eastern Australia. Marine Geology 289, 100–116.
Puga-Bernabeu, A., Webster, J.M., Beaman, R.J., Guilbaud, V., 2013. Variation in canyon morphology on the Great Barrier Reef margin, north-eastern Australia: the influence of slope and barrier reefs. Geomorphology 191, 35–50.
Puga-Bernabeu, A., Webster, J.M., Beaman, R.J., Reimer, P.J., Renema, W., 2014. Filling the gap: a 60 ky record of mixed carbonate-siliciclastic turbidite deposition from the Great Barrier Reef. Marine and Petroleum Geology 50, 40–50.
Puig, P., Greenan, B.J.W., Li, M.Z., Prescott, R.H., Piper, D.J.W., 2013. Sediment transport processes at the head of Halibut Canyon, eastern Canada margin: an interplay between internal tides and dense shelf-water cascading. Marine Geology 341, 14–28.
Ramirez-Llodra, E., Company, J.B., Sarda, F., Rotllant, G., 2010. Megabenthic diversity patterns and community structure of the Blanes submarine canyon and adjacent slope in the Northwestern Mediterranean: a human overprint? Marine Ecology 31, 167–182.
Rennie, S.J., Pattiaratchi, C.B., McCauley, R.D., 2009a. Numerical simulation of the circulation within the Perth Submarine Canyon, Western Australia. Continental Shelf Research 29, 2020–2036.
Rennie, S., Hanson, C.E., McCauley, R.D., Pattiaratchi, C., Burton, C., Bannister, J., Jenner, C., Jenner, M.N., 2009b. Physical properties and processes in the Perth Canyon, Western Australia: links to water column production and seasonal pygmy blue whale abundance. Journal of Marine Systems 77, 21–44.
Ridgway, K.R., Dunn, J.R., 2003. Mesoscale structure of the mean East Australian Current System and is relationship with topography. Progress In Oceanography 56, 189–222.
Robison, B.H., Sherlock, R.E., Reisenbichler, K.R., 2010. The bathypelagic community of Monterey Canyon. Deep Sea Research Part II: Topical Studies in Oceanography 57, 1551–1556.
Roughan, M., Middleton, J.H., 2004. On the East Australian Current: variability, encroachment, and upwelling. Journal of Geophysical Research 109, C07003.
Rowe, G.T., 1971. Observations on bottom currents and epibenthic populations in Hatteras submarine canyon. Deep Sea Research and Oceanographic Abstracts 18, 569–581.
Rowe, G.T., Polloni, P.T., Haedrich, R.L., 1982. The deep-sea macrobenthos on the continental margin of the northwest Atlantic Ocean. Deep-Sea Research Part A: Oceanographic Research Papers 29, 257–278.
Schlacher, T.A., Schlacher-Hoenlinger, M.A., Williams, A., Althaus, F., Hooper, J.N.A., Kloser, R., 2007. Richness and distribution of sponge megabenthos in continental margin canyons off southeastern Australia. Marine Ecology Progress Series 340, 73–88.
Shepard, F.P., 1972. Submarine canyons. Earth-Science Reviews 8, 1–12.
Shepard, F.P., 1975. Progress of internal waves along submarine canyons. Marine Geology 19, 131–138.
Shepard, F.P., 1981. Submarine canyons: multiple causes and long-time persistence. AAPG Bulletin 65, 1062–1077.
Shepard, F.P., Dill, R.F., 1966. Submarine Canyons and Other Sea Valleys. Rand McNally, Chicago, Illinois (381 pp.).
Shepard, F.P., Marshall, N.F., McLoughlin, P.A., 1974a. Currents in submarine canyons. Deep Sea Research 21, 691–706.
Shepard, F.P., Marshall, N.F., McLoughlin, P.A., 1974b. Internal waves advancing along submarine canyons. Science 183, 195–198.
Skene, K.I., Piper, D.J.W., 2006. Late Cenozoic evolution of Laurentian Fan: development of a glacially-fed submarine fan. Marine Geology 227, 67–92.
Skliris, N., Djenidi, S., 2006. Plankton dynamics controlled by hydrodynamic processes near a submarine canyon off NW corsican coast: a numerical modelling study. Continental Shelf Research 26, 1336–1358.
Suthers, I.M., Young, J.W., Baird, M.E., Roughan, M., Everett, J.D., Brassington, G.B., Byrne, M., Condie, S.A., Hartog, J.R., Hassler, C.S., Hobday, A.J., Holbrook, N.J., Malcolm, H.A., Oke, P. R., Thompson, P.A., Ridgway, K., 2011. The strengthening East Australian Current, its eddies and biological effects — an introduction and overview. Deep-Sea Research II 58, 538–546.
Tesi, T., Puig, P., Palanques, A., Goni, M.A., 2010. Lateral advection of organic matter in cascading-dominated submarine canyons. Progress In Oceanography 84, 185–203.
Toussaint, G., 1983. Solving geometric problems with the rotating calipers. Proceedings of IEEE MELECON'83, Athens, Greece, May 1983.
van Oevelen, D., Soetaert, K., Garcia, R., de Stigter, H.C., Cunha, M.R., Pusceddu, A., Danovaro, R., 2011. Canyon conditions impact carbon flows in food webs of three sections of the Nazare canyon. Deep Sea Research Part II: Topical Studies in Oceanography 58, 2461–2476.
Vetter, E.W., 1994. Hotspots of benthic production. Nature 372, 47.
Vetter, E.W., Dayton, P.K., 1998. Macrofaunal communities within and adjacent to a detritus-rich submarine canyon system. Deep Sea Research Part II: Topical Studies in Oceanography 45, 25–54.
Vetter, E.W., Dayton, P.K., 1999. Organic enrichment by macrophyte detritus and abundance patterns of megafaunal populations in submarine canyons. Marine Ecology Progress Series 186, 137–148.
Vetter, E.W., Smith, C.R., De Leo, F.C., 2010. Hawaiian hotspots: enhanced megafaunal abundance and diversity in submarine canyons on the oceanic islands of Hawaii. Marine Ecology 31, 183–199.
Von Der Borch, C.C., 1968. Southern Australian submarine canyons: their distribution and ages. Marine Geology 6, 267–279.
Webster, J.M., Beaman, R.J., Puga-Bernabeu, A., Ludman, D., Renema, W., Wust, R.A.J., George, N.P.J., Reimer, P.J., Jacobsen, G.E., Moss, P., 2012. Late Pleistocene history of turbidite sedimentation in a submarine canyon off the northern Great Barrier Reef, Australia. Palaeogeography, Palaeoclimatology, Palaeoecology 331–332, 75–89.
Whiteway, T.G., 2009. Australian bathymetry and topography grid, June 2009. Geoscience Australia Record 2009/21Geoscience Australia, Canberra (46 pp.).
Wilson, O., 2012. 50 m Multibeam Dataset of Australia. Geoscience Australia. https://www.ga.gov.au/products/servlet/controller?event=GEOCAT_DETAILS&catno=73842 (accessed 10 June, 2013).
Yoklavich, M.M., Greene, H.G., Cailliet, G.M., Sullivan, D.E., Lea, R.N., Love, M.S., 2000. Habitat associations of deep-water rockfishes in a submarine canyon: an example of a natural refuge. Fishery Bulletin 98, 625–641.
Zuniga, D., Flexas, M.M., Sanchez-Vidal, A., Coenjaerts, J., Calafat, A., Jorda, G., Garcia-Orellana, J., Puigdefabregas, J., Canals, M., Espino, M., Sarda, F., Company, J.B., 2009. Particle fluxes dynamics in Blanes submarine canyon (Northwestern Mediterranean). Progress In Oceanography 82, 239–251.

Further reading

Glenn, K., Post, A., Keene, J., Boyd, R., Fountain, L., Potter, A., Osuchowski, M., Dando, N., 2008. NSW Continental Slope Survey- Post Cruise Report. Geoscience Australia Record 2008/14, Canberra 10, 97–110 (160pp.).